HELSINKI UNIVERSITY OF TECHNOLOGY
Faculty of Electronics, Communication and Automation
Department of Radio Science and Engineering

Jari Holopainen

Handheld DVB and Multisystem Radio Antennas

Thesis submitted in partial fulfillment for the degree of Licentiate of Science in Espoo . . 2008.

Supervisor Professor (pro tem) Clemens Icheln

Second examiner Professor Sergei Tretyakov

HELSINKI UNIVERSITY OF TECHNOLOGY

ABSTRACT OF THE LICENTIATE THESIS

Author:	Jari Holopainen
Name of the thesis:	Handheld DVB and Multisystem Radio Antennas
Date:	April 30, 2008 **Number of pages:** 87
Faculty:	Electronics, Communication and Automation
Department:	Radio Science and Engineering
Supervisor:	Professor (pro tem) Clemens Icheln
Second examiner:	Professor Sergei Tretyakov

In this licentiate thesis the implementation of small internal DVB-H antennas for handheld multisystem radios is studied, and several prototypes and simulated designs are presented and evaluated.

Since the volume that can be reserved for antennas is very restricted, the limits for the size of capacitive coupling element based antenna structures inside handsets of different size were studied. The results indicate that the smallest required volume of the coupling element which ensures sufficient performance in today's typical-size monoblock mobile handsets would be about 3 - 4 cm^3. Instead, for tablet-size and open clamshell-size terminals the antenna element are shown to be significantly smaller and thinner. Direct-feed-based structures can provide very low profile antenna solutions for tablet and clamshell-type terminals.

The effect of the user on performance of the DVB-H antenna was studied for some cases. Maximum of 5 - 9 dB decrease in the total efficiency was shown and thus the effect of the user seems to be a significant challenge for the operation of DVB-H. Relatively low isolation, about 18 dB, between the DVB-H and GSM900 antennas was demonstrated and thus the interoperability of DVB-H and GSM900 systems seems impossible without additional filtering.

Keywords: small antennas, internal antenna, coupling structures, capacitive coupling element, direct feed, DVB-H, mobile TV, multisystem radio, effect of user, interoperability

TEKNILLINEN KORKEAKOULU

LISENSIAATTITYÖN TIIVISTELMÄ

Tekijä:	Jari Holopainen
Työn nimi:	Kannettavan DVB-vastaanottimen ja monijärjestelmäradion antennit
Päivämäärä:	30. huhtikuuta 2008 **Sivuja:** 87
Tiedekunta:	Elektroniikan, tietoliikenteen ja automaation tiedekunta
Laitos:	Radiotieteen ja -tekniikan laitos
Työn valvoja:	Ma. professori Clemens Icheln
Toinen tarkastaja:	Professori Sergei Tretyakov

Tässä lisensiaattityössä on tutkittu sisäisen DVB-H-antennin toteuttamista monijärjestelmäpäätelaitteessa ja esitetty muutamia antenniprototyyppejä ja simuloituja antennikonstruktioita.

Koska antenneille varattu tila päätelaitteen sisällä on rajallinen, työssä on tutkittu pienimmän mahdollisen kytkentäelementtiin perustuvan antennin vaatimaa tilavuutta erikokoisissa päätelaitteissa. Tutkimuksen tuloksena esitetään, että riittävään suorituskykyyn tyypillisen kokoisessa päätelaitteessa päästään kytkentäelementillä, jonka tilavuus on noin 3 - 4 cm^3. Tabletti- ja avonaisessa simpukkapäätelaitteessa riittää tilavuudeltaan ja korkeudeltaan huomattavasti kompaktimpi antennielementti tai suorasyöttörakenne.

Työssä tutkittiin myös käyttäjän vaikutusta DVB-H-antennin toimintaan. Simuloimalla tehty tutkimus osoitti, että käyttäjä voi aiheuttaa jopa 5 - 9 desibelin häviöt kokonaishyötysuhteeseen. Simuloidussa esimerkkikonstruktiossa osoitettiin, että DVB-H- ja GSM900-antennien välillä on noin 18 desibelin isolaatio, joka ei riitä takaamaan järjestelmien samanaikaista toimintaa, vaan isolaatiota jouduttaisiin kasvattamaan muilla keinoilla.

Avainsanat: pienet antennit, sisäinen matkapuhelinantenni, kytkentärakenne, kapasitiivinen kytkentäelementti, suorasyöttörakenne, DVB-H, mobiili-TV, käyttäjän vaikutus, yhteentoimivuus

Preface

The following persons and organizations deserve my deepest gratitude:

Professors Pertti Vainikainen, Clemens Icheln and Sergei Tretyakov

Outi Kivekäs, Juha Villanen, Mikko Kyrö and Juho Poutanen

language assistant Jani

workmates Antti, Aleksi, Maria, Olli, Pekka and Tero at the Department of Radio Science and Engineering

parents Mirja and Juhani and sister Hanna
friends, above all Pasi

Graduate School of Electrical and Communications Engineering,
Nokia foundation, HPY:n tutkimussäätiö

Otaniemi, Espoo, May Day's Eve 2008

Jari Holopainen

Contents

Abbreviations

CCE	Capacitive coupling element
DVB	Digital video broadcast
DVB-H	Digital video broadcast - handheld
DVB-T	Digital video broadcast - terrestrial
DF	Direct feed
EMC	Electromagnetic compatibility
FDTD	Finite difference time domain
GPRS	General packet radio service
GPS	Global positioning system
GSM	Global system for mobile communication
IC	Integrated circuit
LNA	Low noise amplifier
MEG	Mean effective gain
N77	Nokia N77, example of multisystem radio
PEC	Perfect electric conductor
PCB	Printed circuit board
PIFA	Planar inverted-F antenna
RLC	Resistor inductor capacitor
SAR	Specific absorbtion rate
TKK	Helsinki University of Technology
UHF	Ultra high frequency
UMTS	Universal mobile telecommunications system
WLAN	Wireless local area network

List of symbols

a	radius of a sphere
B	susceptance
B_r	relative bandwidth
$B_{r,max}$	maximum relative bandwidth
$B_{sr,max}$	maximum relative bandwidth in single-resonant case
$B_{dr,max}$	maximum relative bandwidth in double resonant case
BVR	bandwidth-to-volume ratio
BW	bandwidth
c_0	speed of light
C	capacitance
d	distance
D	directivity
E_{inc}	electric field strength
f	frequency
f_r	resonant frequency
f_{rc}	resonant frequency of chassis
G	conductance
G_r	realized gain
h	height of coupling element
k	coupling factor
k_{opt}	optimal coupling factor
k_0	wave number in free space
l	length (of chassis)
l_{CCE}	length of coupling element

L	inductance
L_{retn}	return loss
P	power
P_0	total (accepted) power
P_{in}	available input power
P_{rad}	radiated power
P_{rec}	sensitivity of receiver
Q	quality factor
Q_0	unloaded quality factor
Q_c	quality factor for conductivity losses
Q_d	quality factor for dielectric losses
Q_{rad}	radiation quality factor
$Q_{rad,min}$	fundamental lowest limit of radiation quality factor
R	resistance
RL	return loss
S	highest acceptable voltage standing wave ratio
T	coupling
$VSWR$	voltage standing wave ratio
W	energy
X	reactance
Z_l	complex load impedance
Z_0	characteristic impedance
η_m	matching efficiency
η_{rad}	radiation efficiency
η_{tot}	total efficiency
η_0	wave impedance
λ	wavelength
λ_0	wavelength in free space
ρ	reflection coefficient
σ	electrical conductivity

Chapter 1

Introduction

Recently, there has been a significant increase in the number of different functions and radio systems built into handheld devices. Traditionally, mobile terminals have included only GSM systems. Today, we have introduced many other radio systems in mobile terminals, e.g. FM radio, digital television (DVB-H), UMTS, GPS, Bluetooth and WLAN. All the systems need an antenna over the operation band. At the same time consumers prefer internal antennas and they want that the size of the terminal remains the same or gets even smaller. Since the volume, which can be reserved for antennas, is limited inside a mobile terminal, it is challenging to integrate all the antennas needed for the different systems inside the handset and to additionally ensure simultaneous operation of different systems. To be able to do that, novel antenna concepts are needed.

Figure 1.1 presents an example of a commercial terminal, Nokia N77 [1], and the radio systems, which could be supported by today's mobile handsets. The dimensions of N77 are 111 mm x 50 mm x 18.8 mm [length x width x maximum thickness]. The frequency bands for the radio systems are presented in Table 1.1 and illustrated in Figure 1.2. Throughout the work, N77 is treated as an example of a multisystem terminal.

Figure 1.1: Nokia N77 and radio systems, which could be integrated into a mobile terminal. N77 includes only DVB-H(EU), GSM900, GSM1800/1900 and UMTS.

Table 1.1: The frequency bands and relative bandwidths (BW) of the radio systems, which could be in a handheld device.

system	freq. [MHz]	BW [MHz]	center freq. [MHz]	BW [%]
FM radio	87.5 - 108	20.5	97.75	21
DVB-H (EU)	470 - 750	280	610	46
GSM 850	824 - 894	70	859	8.1
GSM 900 (E-GSM)	880 - 960	80	920	8.7
GPS	1575.42 (1227.60)			< 2
GSM 1800	1710 - 1880	170	1795	9.4
GSM 1900	1850 - 1990	140	1920	7.3
UMTS	1920 - 2170	250	2045	12.2
Bluetooth / WLAN	2400 - 2500	100	2450	4.1

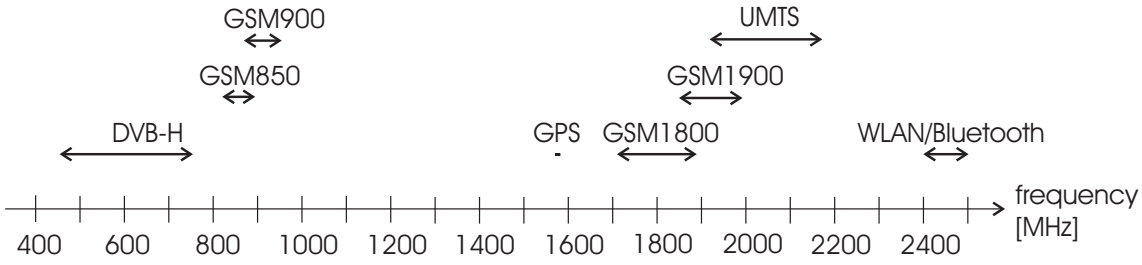

Figure 1.2: The frequency bands of the radio systems could be in a handheld device.

DVB-H is a new service, which brings data broadcasting[1] into handheld terminals. It is an adapted version of the terrestrial digital television (DVB-T) enabling special features such as lower power consumption, smaller antenna, Doppler effect tolerance, better indoor reception and smoother handovers, all of which are important in mobile applications.

DVB-T reception usually exploits either rooftop Yagi-Uda antennas or desktop whip antennas. Since commercial success for DVB-H was not expected with fairly large external antennas, most terminal manufacturers have decided to build antennas inside their products. Reducing the size (say, from rather large DVB-T antennas to obviously smaller internal DVB-H antennas) affects remarkably the performance of the antenna. However, 'an engineering solution' is not to provide very high electrical performance for the antenna and thus compromise with other important characteristics such as the size of the antenna. Therefore, the performance of the antenna is reduced to the level that is just enough for guaranteeing the operation of the whole system with a certain reliability level. Sacrificing the performance makes it possible to decrease the size of the antenna to be feasible in today's mobile terminals.

The goal of this work is to present a comprehensive study of the implementation of DVB-H antennas inside a mobile terminal. First, a review of available DVB-H antennas is done. Then the limits for the smallest possible DVB-H antenna structures are studied. As aresult, several novel antenna designs are presented. In addition, the effect of the user on the DVB-H antenna operation is examined. Since DVB-H is supposed to operate in a multisystem radio, the interoperability of the DVB-H antenna with other antennas is investigated, too.

This thesis is organized as follows. Small-antenna fundamentals, matching circuits as well as bandwidth enhancement methods are briefly discussed in Chapter 2. Chapter 3 introduces compact coupling structures that are very usable for the antennas of

[1]Data broadcasting, or briefly datacasting, provides programs, news, weather forecasts, movies, music, games, traffic, shopping, education and other public services for many users with a point to multipoint service. The service is possibly interactive, the return channel implemented over GPRS or UMTS.

the systems operating at the lower UHF frequencies such as DVB-H and GSM900. Chapters 2 and 3 are important for recognizing the challenges behind the DVB-H antenna implementation and for understanding the antenna solutions presented in Chapter 4. According to the author's knowledge, Chapter 3 is also the first published comprehensive collection of data on compact coupling structures. Chapter 4 is the main chapter of the work. It introduces design aspects of DVB-H antennas, reviews existing antenna solutions, and presents novel designs based on the compact coupling structure concept. The effect of the user of DVB-H antennas and the interoperability of the DVB-H antenna with different transmitting systems in the same terminal are also presented in the end of Chapter 4. The summary of the work is presented in Chapter 5, and Chapter 6 is for the final conclusions and future outlook.

The results of this thesis are collected from the work carried out by the author at the Department of Radio Science and Engineering (until 2008, Radio Laboratory) of Helsinki University of Technology since June 2005. The work is direct continuation of the author's Master's thesis 'Antenna for Handheld DVB Terminal' published in May 2005 [2].

Chapter 2

Small-antenna fundamentals, matching circuits and bandwidth enhancement methods

An antenna can be defined as 'small' in different ways. In this work, small antennas are understood as *electrically* small antennas, which means that they can be enclosed inside a sphere of radius $a = \lambda_0/2\pi$, where λ_0 is the free space wavelength at the operating frequency [3]. This chapter presents basic theory and factors that are used for describing small antennas. In addition, basic matching methods as well as some bandwidth enhancement methods are discussed.

2.1 Small antenna as a resonator

In the reactive near fields of small antennas much more energy is stored than it is radiated in the far field in a period. The near fields consist of the inductive and capacitive parts and the energy oscillates between the magnetic and electric fields. The resonance is achieved when the inductive and capacitive energy levels are equal. Since the operation of small antennas is based on the resonance phenomenon, it is advantageous to use the well-known resonator theory in the antenna design.

The quality factor Q describes the ratio between the energy W stored and the energy P dissipated per time unit in the resonator. The general definition of the quality factor is [4]

$$Q = \frac{2\pi f_r W}{P}. \tag{2.1}$$

Different quality factors can be defined. The unloaded quality factor Q_0 describes all the losses P_0 in the resonator. The losses are generated in the metallic and dielectric parts but also due to the radiation propagating outside the resonator. Radiation quality factor Q_{rad} describes the power radiated by the resonator. The dielectric and conductor losses are described by dielectric and conductor quality factors Q_d and Q_c that can be estimated using formulas given in [5]. The connection between the different quality factors is [4]

$$\frac{1}{Q_0} = \frac{1}{Q_{rad}} + \frac{1}{Q_c} + \frac{1}{Q_d}. \tag{2.2}$$

There is a fundamental lowest limit for the radiation quality factor of an antenna. If the antenna is enclosed inside a sphere with the radius a and it stores no energy inside the sphere, the smallest possible radiation quality factor of a linearly polarized antenna radiating at the lowest TE or TM resonance mode can be calculated from [6] [7] [8]:

$$Q_{rad,min} = \frac{1}{k_0 a} + \frac{1}{(k_0 a)^3} \tag{2.3}$$

where the wave number $k_0 = \frac{2\pi}{\lambda_0}$ and λ_0 is the free space wavelength. Because of the above ideal assumptions, it is not possible to reach $Q_{rad,min}$ in practice.

A small antenna accepts the largest amount of power at the resonant frequency. Outside the resonant frequency the impedance of a small antenna changes rapidly and due to that the impedance becomes the main factor, which limits the usable bandwidth. The impedance bandwidth is usually defined in terms of the voltage standing wave ratio, $VSWR$, or return loss, L_{retn}. The typical criteria for the bandwidth antennas are $VSWR \leq 2$ or $L_{retn} \geq 10$ dB. Near the resonant frequency, the impedance of a small antenna can be modeled as a series or parallel RLC equivalent circuit. The relative impedance bandwidth of the equivalent circuit can be easily derived and it can be calculated from

$$B_r = \frac{1}{Q_0}\sqrt{\frac{(TS-1)(S-T)}{S}}. \tag{2.4}$$

where S is the maximum accepted voltage standing wave criterion at the edges of the impedance band and T is the coupling coefficient [9].

As well known, instead of having perfect matching at the center frequency (critical coupling, $T = 1$) one can use optimal overcoupling to maximize the bandwidth [9]. The theoretical maximum bandwidth $B_{sr,max}$ of a single-resonant antenna can be derived from (2.4) by finding the maximum for the bandwidth using the differential calculus:

$$B_{sr,max} = \frac{S^2 - 1}{2SQ_0}. \tag{2.5}$$

2.2 Efficiency

Radiation efficiency is defined as the ratio of the power radiated P_{rad} and the power P_0 accepted by the antenna [10]:

$$\eta_{rad} = \frac{P_{rad}}{P_0} = \frac{Q_0}{Q_{rad}}. \tag{2.6}$$

Matching efficiency is defined as the ratio between the power P_o accepted and the power P_{in} available at the antenna input [10]:

$$\eta_m = \frac{P_0}{P_{in}} = 1 - |\rho|^2, \tag{2.7}$$

where ρ is the voltage reflection coefficient. For example, if the return loss is 10 dB at the edges of the impedance band, the corresponding reflection coefficient is about $|\rho| = 0.316$ and thus the matching efficiency over the impedance band is $\eta_m \geq 0.90$. Total efficiency η_{tot} is the product of the radiation and matching efficiencies [10]:

$$\eta_{tot} = \eta_{rad} \cdot \eta_m. \tag{2.8}$$

2.3 Basic matching methods

To guarantee sufficient power transmission between the antenna and the feed line, the antenna needs to be matched to the impedance of the feed line, i.e. the antenna

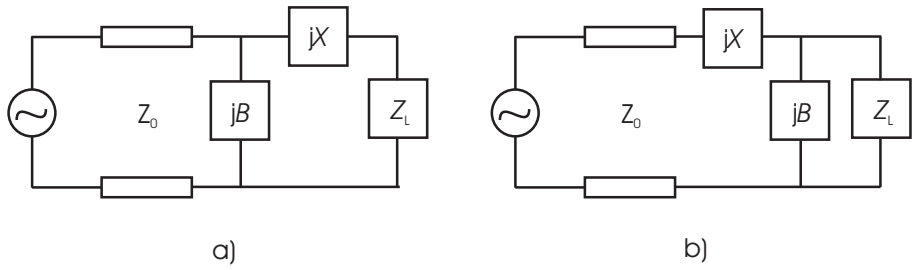

Figure 2.1: L section matching networks.

resonance has to be achieved. Antennas are either self-resonant or the resonance is produced with an external matching circuitry. Typical self-resonant antennas are open $\lambda/2$ resonators (like dipole and half-wave microstrip antennas) and short-circuited $\lambda/4$ resonators (like monopole, helix and PIFA). If the matching is not sufficient, or if the resonance needs to be tuned, a matching circuitry is needed.

Below 1 GHz, lumped elements, such as capacitors and inductors, are applicable in matching circuits because they operate fairly ideally [4], [11]. Depending on the lumped components, they can also be used at higher frequencies if the physical size of the component is clearly smaller than the wavelength (i.e. the largest dimension is smaller than e.g. $\lambda/30$ [5]) and the ohmic losses and parasitics are small enough.

Basic lumped element matching circuits consist of L-section networks [4], [11], see Figure 2.1. Z_l is the complex impedance to be matched, j is the imaginary unit, X is the reactance of the component, which can be either a capacitor or an inductor, B is the susceptance that is also a capacitor or an inductor and Z_0 is the characteristic impedance of the feed line. Any impedance with the real part larger than zero can be matched. The topology of the matching circuit (8 possibilities) is defined by the location of the load impedance Z_l on the Smith chart [4], see Figure 2.2. The designer can basically choose from two or four suitable matching circuit topologies but the impedance bandwidth achieved depends on the topology chosen [11]. The design of basic matching circuits is presented e.g. in [4], [11].

At higher frequencies, where lumped elements do not operate very ideally due to parasitics and losses, the matching circuitry can be realized using distributed elements such as tuning stubs or a quarter-wavelength transformer. The distributed

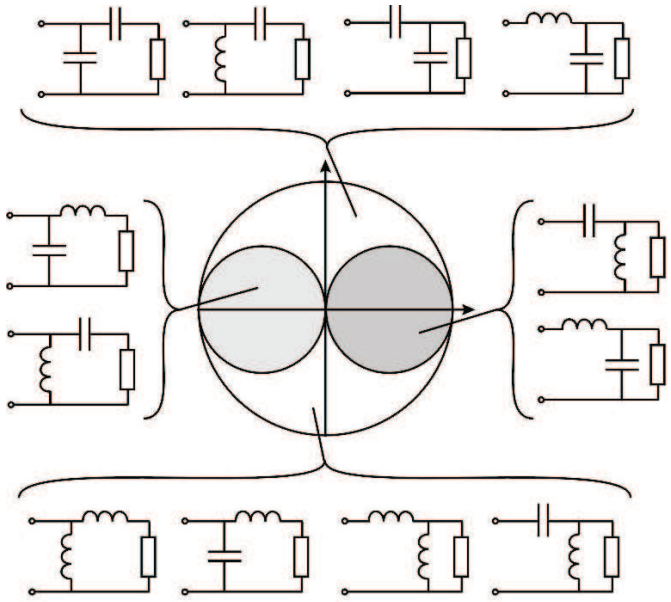

Figure 2.2: Matching circuit topology dependence on the location of the load impedance on the Smith chart [4].

elements can be used at lower frequencies too, but the size of the matching circuit may usually become too large. The design of basic distributed elements matching circuits is also presented in [4], [11].

2.4 Bandwidth enhancement

The inherently narrow bandwidth of small antennas could, in principle, be enhanced e.g. by increasing the volume of the antenna, see (2.3), (2.4) and (2.6). That is not feasible in modern mobile phones in which the volume reserved for the antennas is limited and the volume cannot be increased, rather the opposite. If the volume is kept the same and the total efficiency decreases, the bandwidth increases, see (2.4), (2.6), (2.7) and (2.8). In this case valuable battery power turns into losses which is contrary to the desired long operation time[1]. Thus, the three important characteristics (bandwidth, efficiency and volume) of a small mobile terminal an-

[1]In addition to this, losses turn into heat, which is both uncomfortable for the user and can damage the most sensitive components (such as IC chips, battery etc.) of the handset.

tenna are interrelated, and a reasonable trade-off has to be found. It is possible to increase (optimize) bandwidth using ways that result in more overall benefits than disadvantages. Those methods are presented in the following sections.

2.4.1 Multi-resonant operation

So far, small antennas have been discussed as single-resonant resonators. Instead of having a single-resonance operation, it is well known that using multiple resonances is a very efficient way to increase the impedance bandwidth. That can be done by adding low-loss resonators into the antenna structure or matching circuitry [12]. Typical single-resonant and dual-resonant responses are shown in Figure 2.3.

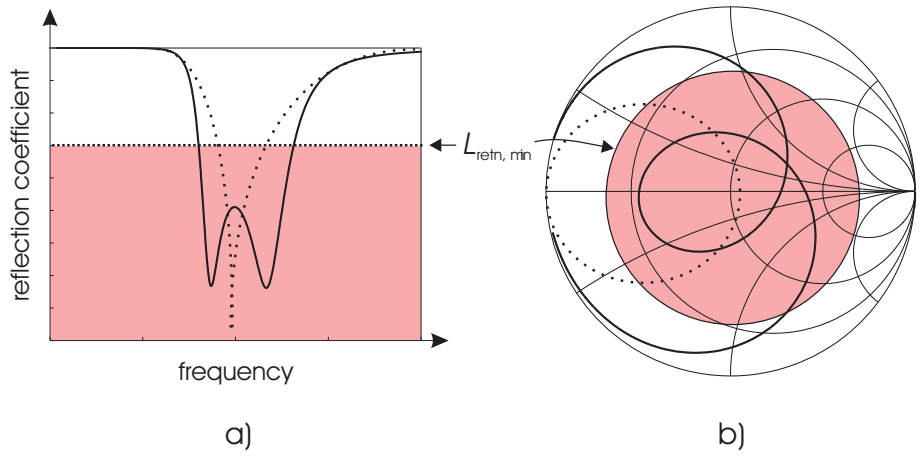

Figure 2.3: Typical single-resonant (dotted) and dual-resonant (solid) responses a) in the Cartesian coordinate system and b) on the Smith chart.

The theoretical maximum bandwidth with an ideal matching circuit containing infinite number of additional resonators ($n = \infty$) can be calculated from the Bode-Fano criterion [11] [13] [14]

$$B_{r,max} = \frac{\pi}{Q_0 \ln(\frac{S+1}{S-1})}, \tag{2.9}$$

where S is the maximum allowed voltage standing wave ratio at the edges of the impedance band, i.e. $VSWR \leq S$.

According to [12], the theoretical maximum bandwidth of a dual-resonant antenna

$(n = 2)$ can be calculated from

$$B_{dr,max} = \frac{\sqrt{S^2 - 1}}{Q_0}. \tag{2.10}$$

According to (2.5) and (2.10), the theoretical maximum bandwidth enhancement with one additional resonator is about 100%, which means doubled bandwidth. With two and three additional resonators the enhancement is about 150% and 180%, respectively, see Figure 2.4. With four or more resonators, the additional benefit gained by each resonator saturates fast towards the theoretical maximum bandwidth given by the Bode-Fano criterion. Also, in practice one or two additional resonators are still feasible, with more resonators the antenna structure or matching circuitry becomes rather complicated.

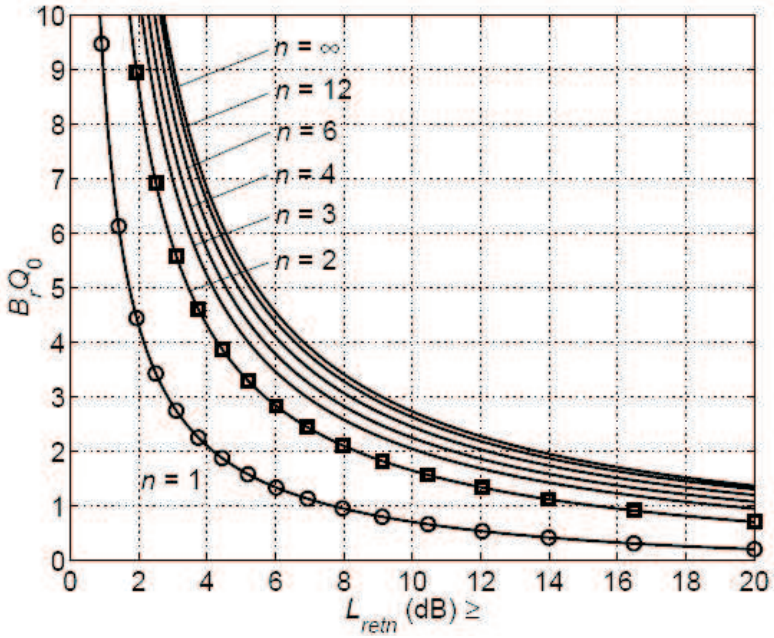

Figure 2.4: Theoretical maximum relative bandwidth B_r with a certain unloaded quality factor Q_0 with $n-1$ additional resonators as a function of the return loss matching criterion [15].

In [12] it has been demonstrated that for self-resonant microstrip antenna structures an additional resonator can be realized e.g. by placing a parasitic patch over or next to the driven patch. The additional resonators (consisting of lumped reactive elements or tuning stubs) can also be implemented in the matching circuitry.

Unlike in the case of single-resonant matching circuits, the design of multi-resonant matching circuits is not very straightforward since general closed-form design formulas do not exist. Only in some special cases, design formulas are available. For example, for an antenna that can be modeled as a series RLC equivalent circuit over a narrow bandwidth, a dual-resonant matching circuit can be designed using analytical design formulas presented in [16].

In practice, traditional filter design principles can also be applied to multi-resonant matching circuit design [17]. First, the input impedance Z_l of an antenna is matched to the terminal impedance at the center frequency of the desired band with an L-section matching circuit, see Figures 2.1 and 2.2. Next, additional resonators can be designed using e.g. the Chebychev design charts, see e.g. [17]. Usually, the component values of the multi-resonant matching circuitry require some tuning and iteration rounds. For that purpose a circuit simulator can be used. Figure 2.5 presents a general topology for a Chebychev-type multi-resonant matching circuitry. The first additional resonator can be either in parallel (the resonator consisting of components C_1 and L_1) or in series (the resonator consisting of components C_2 and L_2). After all, the matching circuits with ideal components provide basis for further design of real matching circuits.

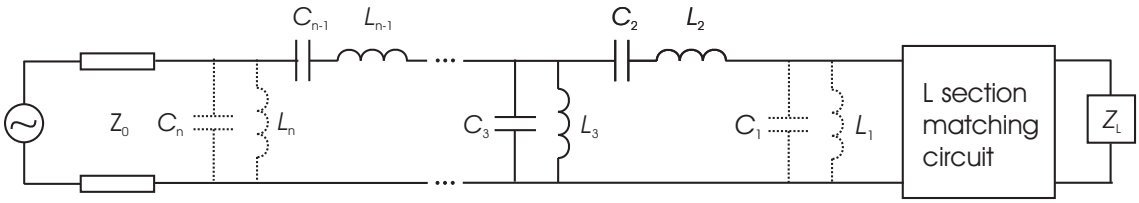

Figure 2.5: General Chebyshev-type multi-resonant matching circuit with n additional resonators.

2.4.2 Sacrificing efficiency

As presented earlier, the impedance bandwidth increases if the total efficiency decreases. It is not recommended but sometimes the total efficiency has to be sacrificed in order to optimize other characteristics such as the size of an antenna. There are three methods how the total efficiency can be reduced artificially.

Firstly, one can use lossy dielectrics in the antenna structure or lossy components (such as resistors) in the matching circuitry. Secondly, an attenuator can be placed between the antenna and the feed line. The third, and easiest option from the antenna designer's point of view, is to allow higher mismatch, i.e. higher voltage standing wave ratio (or smaller return loss) at the edges of the impedance band. When comparing to the other methods, acceptance some mismatch can be shown to provide the largest bandwidth with a certain total efficiency, see [2]. However, the highest acceptable voltage standing wave ratio depends on the electronics and the signal processing method used in the system because the reflections from the antenna may cause oscillations in the power amplifier and distortion in signals (and consequently bit errors).

To be able to keep the volume occupied by the antenna as low as possible, moderate mismatching is already now allowed in current mobile phones. Instead of having the traditional 10 dB return loss matching criterion, 6 dB is used in the cellular systems, see e.g. [15]. When accepting the 6 dB criterion, the bandwidth increases theoretically about 78% in a single-resonant case, see (2.5), and 63% in a dual-resonant case, see (2.10), compared to the 10 dB criterion. The price paid is 17% lower total efficiency at the edges of the impedance band, see (2.7) and (2.8).

Chapter 3

Compact coupling structures

The ground planes of the printed circuit board (PCB), EMC shieldings and other metal plates (like display) of a handheld device create a solid RF counterpoise, briefly called chassis. This electrically conductive chassis has significant effect on the antenna operation. Actually, the required bandwidth of current small internal antennas would not be possible without the presence of the chassis at lower UHF frequencies, i.e. below 1 GHz, because the representative antenna element would be electrically too small to be able to cover the bandwidths required for DVB-H and GSM900. In this chapter it is presented how the chassis can be exploited as a part of the antenna structure when applying compact coupling structures.

3.1 PIFA on a finite chassis

Figure 3.1a presents a PIFA antenna on a 100 mm x 44 mm [length x width] chassis, which is here modeled as a thin high-conductivity metal sheet. The volume occupied by the PIFA is 7.1 cm^3. The antenna structure was studied with a method of moments based electromagnetic simulator IE3D by Zeland [18]. The reflection coefficient is presented in Figure 3.1b.

According to Figure 3.1, the 6 dB return loss band of the antenna is 0.874 - 0.979 GHz and the relative bandwidth is then 11.3%. The radiation efficiency η_{rad} is about 96%

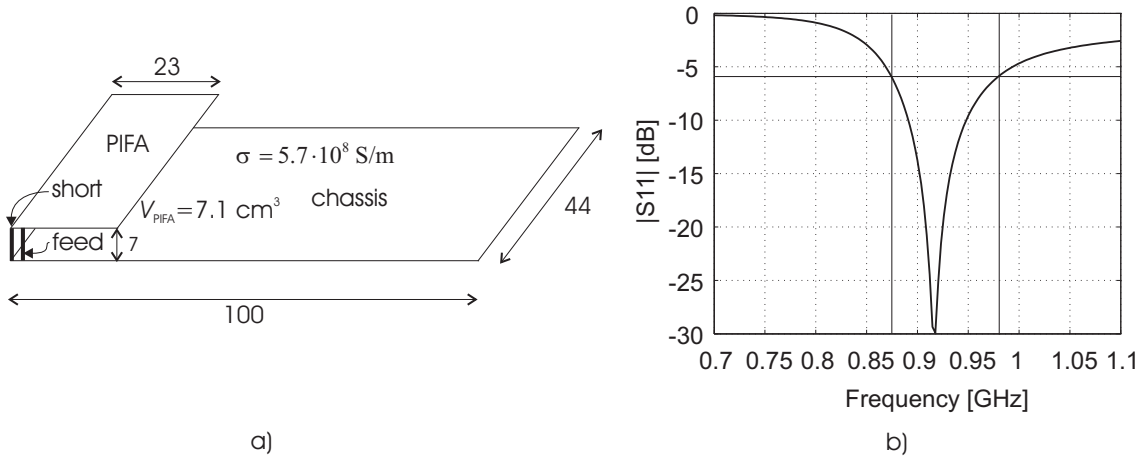

Figure 3.1: PIFA element on a finite chassis and the reflection coefficient of the antenna structure.

(includes only metal losses). The radiation quality factor can be calculated using (2.4) and (2.6), now $S = 3.0$ and $T = 1$:

$$Q_{rad} = \frac{1}{B_r \eta_{rad}} \frac{S-1}{\sqrt{S}} = 10.68. \tag{3.1}$$

In order to calculate the fundamental lowest limit of the radiation quality factor of the PIFA, the element is placed within a sphere having the radius of

$$a = \frac{\sqrt{23^2 + 44^2 + 7^2}}{2} \text{ mm } = 25.07 \text{ mm}. \tag{3.2}$$

At the center frequency of the antenna (0.9266 GHz) the wavelength is 0.3236 m. Thus, the wave number in free space is $k = \frac{2\pi}{\lambda_0} = 19.42$ 1/m. The fundamental lowest limit of the radiation quality factor can then be calculated from (2.3):

$$Q_{rad,min} = \frac{1}{ka} + \frac{1}{(ka)^3} = 10.72. \tag{3.3}$$

The radiation quality factor of the PIFA seems to be approximately equal to the fundamental lowest limit. As discussed earlier it is in practise not possible to get even close to the limit. Thus, one cannot expect that the PIFA is the only radiator. If one takes a look at a simulated current distribution of the whole structure at 900 MHz, see Figure 3.2, one can notice that there are also relatively strong currents along the long edges of the chassis.

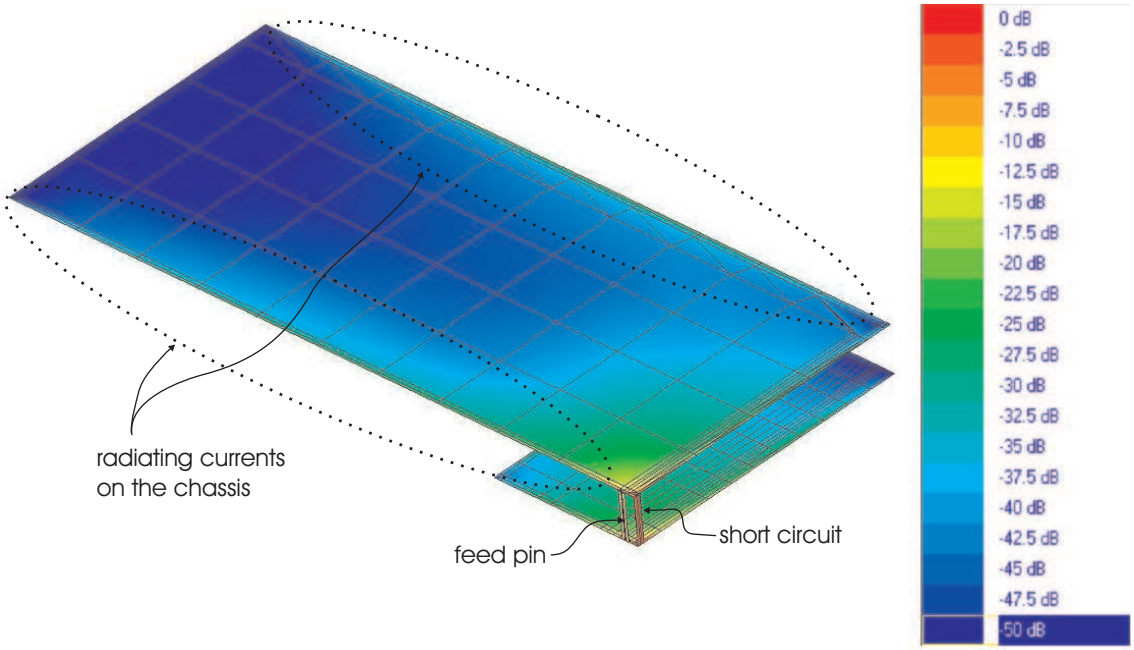

Figure 3.2: Current distribution of the PIFA antenna element and the chassis simulated at 900 MHz with IE3D.

Thus, the currents on the chassis also contribute to the radiation and the fundamental lowest limit of the radiation quality factor has to be estimated for the whole structure including the chassis. In this case the antenna structure is placed within a sphere with the radius of $a = \sqrt{100^2 + 44^2 + 7^2}/2$ mm $= 54.74$ mm. The fundamental lowest limit of the radiation quality factor is then $Q_{rad,min} = 1.77$. Eventually the radiation quality factor of the antenna is clearly larger than the fundamental lowest limit and the theory and simulated results agree. Actually, it has been shown in [19] that the chassis is the main radiator below 1 GHz. At 900 MHz, more than 90% of the radiation is contributed by the chassis. At 2 GHz, the antenna element radiation becomes more significant, about 50% of the radiated power is contributed by the antenna element [19].

3.2 Compact coupling structures

Traditional mobile terminal antennas, such as PIFA, create the antenna resonance and couple currents to the surface of the chassis. A part of the antenna element

volume is needed for creating the resonance and a part is needed for coupling the currents to the chassis. Since the antenna element itself is only a minor radiator below 1 GHz, the volume occupied by the element can be decreased remarkably by introducing compact coupling structures whose principal function is only to couple currents to the chassis. The resonance is then created with a separate matching circuitry outside the coupling element. Figure 3.3a presents such structure that occupies the volume of only 2.0 cm^3. The antenna structure including the matching circuitry, which creates resonance at 900 MHz, is simulated with IE3D. The reflection coefficient is shown in Figure 3.3b.

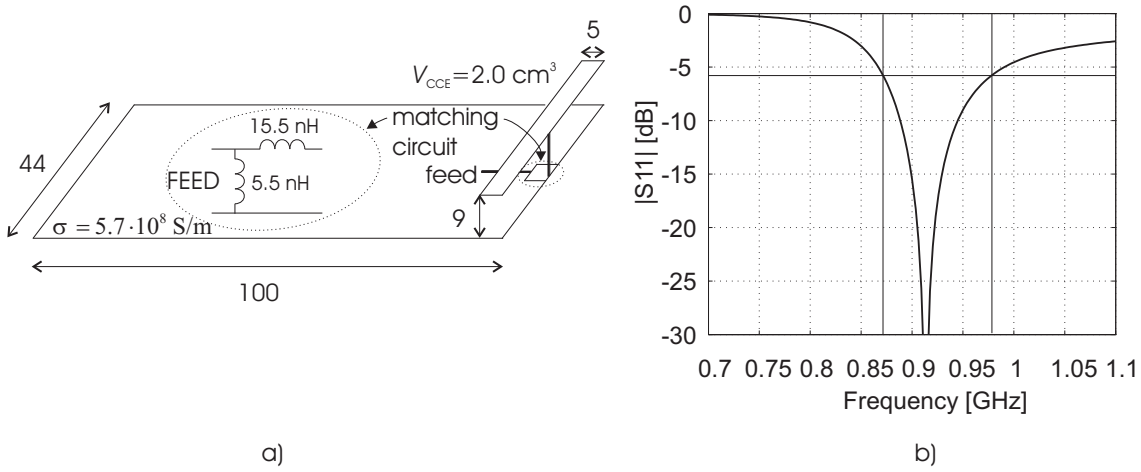

Figure 3.3: a) Compact coupling element antenna structure including the matching circuit and b) the reflection coefficient.

According to Figure 3.3b, the 6 dB return loss band is 0.873 - 0.976 GHz, the relative bandwidth being then 11.1%. When comparing with the PIFA antenna in Figure 3.1, the relative bandwidth is approximately the same but the volume occupied by the coupling element is about 72% smaller than the volume occupied by the PIFA element. Since the bandwidth-to-volume ratio (BVR) of the compact coupling element structure is much larger than the BVR of the PIFA antenna (coupling element: 5.6%/cm^3, PIFA: 1.6 %/cm^3), PIFA antennas are not optimal when considering the ratio of the available bandwidth versus volume occupied.

There are different coupling structures that are categorized according to the way the coupling is done. The currents on the surface of the chassis can be created via electric or magnetic fields or using galvanic coupling. The different coupling methods

and related compact coupling structures are illustrated in Figure 3.4. Coupling via electric fields can be implemented using a capacitive coupling element, briefly CCE, Figure 3.4a. Another capacitive coupling element was already shown in Figure 3.3. An inductive coupling loop[1], briefly ICL, couples via magnetic fields, see Figure 3.4b. A galvanic feed can be created using a direct feed across a high-impedance gap, DF, see Figure 3.4c.

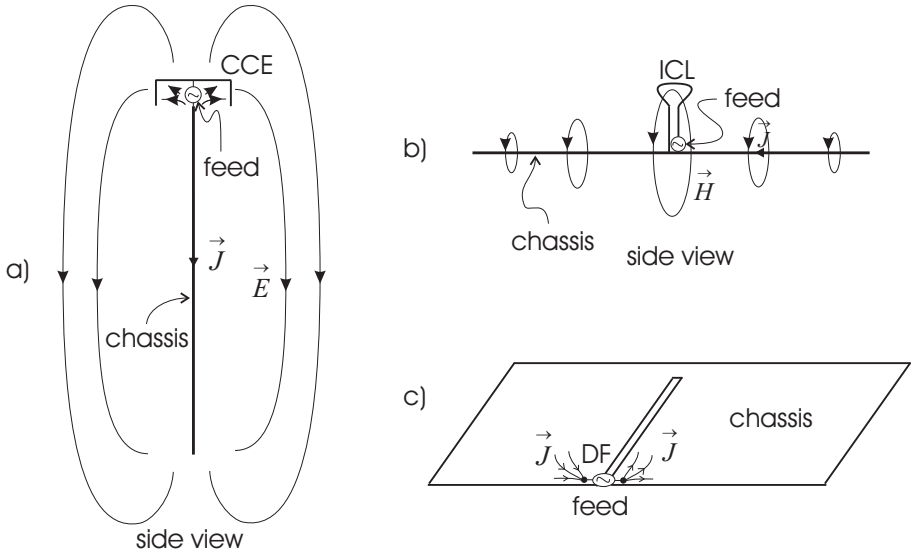

Figure 3.4: a) Capacitive coupling element (CCE), b) inductive coupling loop (ICL) and c) direct feed (DF). E is the electric field, H is the magnetic field and, J is the electric current.

There are many advantages when using compact coupling structures. As presented, they are compact in size. They are also fairly flexible for an antenna designer since the antenna resonance is created with the matching circuitry and because of that, the type, location and shape of the coupling structure can be optimized according to the coupling purpose. The resonant frequency of the antenna is separately chosen with a suitable matching circuit. Usually, the bandwidth enhancement methods presented in the previous chapter are also used to broaden the achievable bandwidth.

[1]Inductive coupling loops have been reported e.g. in [20] but those are not handled in this work.

3.3 Wavemodes and resonator-based analysis

This section will introduce how the combination of the feed structure and the chassis can be modeled and understood using the well-known resonator theory. A rectangular chassis supports a thick-dipole type current distribution and has certain resonant frequencies. The lowest order resonance, or wavemode, exists when the currents flow along the major axis of the chassis that is electrically $\lambda/2$ long, i.e. the current distribution half-wave [19], [21]. The lowest order resonant frequency f_{rc} of the chassis (having the width of 40 mm) can be estimated using the equation given in [19]:

$$f_{rc} \approx (0.73...0.78)\frac{c_0}{2l}, \tag{3.4}$$

in which c is the speed of light and l is the length of the chassis. Since the current distribution of the chassis is dipole-type, the electric fields pattern radiated by the chassis are also similar to those of a dipole antenna. Especially, at the lower UHF frequencies the lowest order wavemode is dominant. The second resonance is reached with electrically λ - length chassis. In this work these first two resonances shall be of interest, other higher wavemodes have been discussed e.g. in [21]. Outside the wavemode frequencies the current distribution is the superposition of the adjacent modes.

As presented in the previous section, compact coupling structures, such as capacitive coupling element or direct feed, couple currents to the chassis, i.e. they can be utilized to effectively excite the chassis wavemodes. Over a narrow frequency band that kind of antenna structures can be studied using two coupled lumped-element resonators. A dipole-type antenna structure, like the chassis, is modeled with a series RLC equivalent circuit. The series RLC circuit is coupled through an ideal transformer to a parallel RLC equivalent circuit which models the coupling structure. The transformer models the coupling between the coupling structure and the chassis. The coupled resonators system is connected to the matching circuitry and finally to the antenna feed. The equivalent circuit of the combination of the feed structure and the chassis is shown in Figure 3.5 and it is studied in detail in [19].

The equivalent circuit can be used only near the resonant frequency of the chassis.

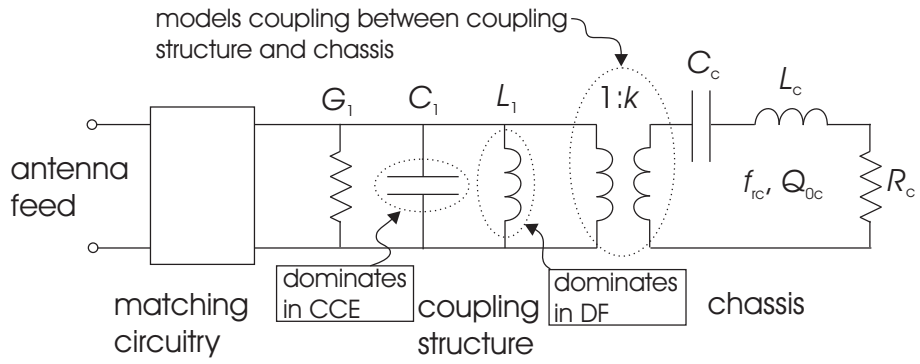

Figure 3.5: Narrowband equivalent circuit of compact coupling structures.

The component values R_c, L_c and C_c can be estimated using the resonant frequency f_{rc} and quality factor Q_{0c} of the chassis. In [19] and [21], it has been reported that the unloaded quality factor Q_{0c} of the chassis at the $\lambda/2$ wavemode resonant frequency is about 2 - 3. At the λ wavemode resonant frequency the unloaded quality factor Q_{0c} is about 3 - 4. The voltage ratio of the transformer k is called the coupling factor. The stronger the coupling, the larger k and vice versa. Components G_1, C_1 and L_1 model the coupling structure. If the capacitive coupling element is applied, the capacitor C_1 dominates over L_1, and vice versa in the case of the direct feed. Finally, the matching is achieved with a suitable matching circuit that can be designed using the methods presented in Chapter 2.

The frequency response of the reflection coefficient of the coupled resonators in Figure 3.5 can be either single-resonant or multi-resonant depending on the strength of the coupling (k) and the difference between the matching and chassis wavemode resonance frequencies (f_m and f_{rc}). Thus, there is a motivation to study systematically the effect of the coupling between the feed structure and the chassis wavemode on achievable bandwidth. The study was conducted using the coupled resonators equivalent circuit presented in Figure 3.5. In this analysis normalized component values were used, the chassis resistor R_c is 1 (Ω), the chassis wavemode resonant frequency f_{rc} is 1 (Hz) and the unloaded quality factor Q_{0c} of the chassis is 2π. Without limiting the generality of the study, the feed structure was modeled as a lossless capacitive coupling element, the capacitance value C_1 is 60m (F), L_1 was infinity and G_1 zero. Frequency responses of the reflection coefficient of the coupled resonators with a suitable L-section matching circuit with different coupling factors

k are presented in Figure 3.6.

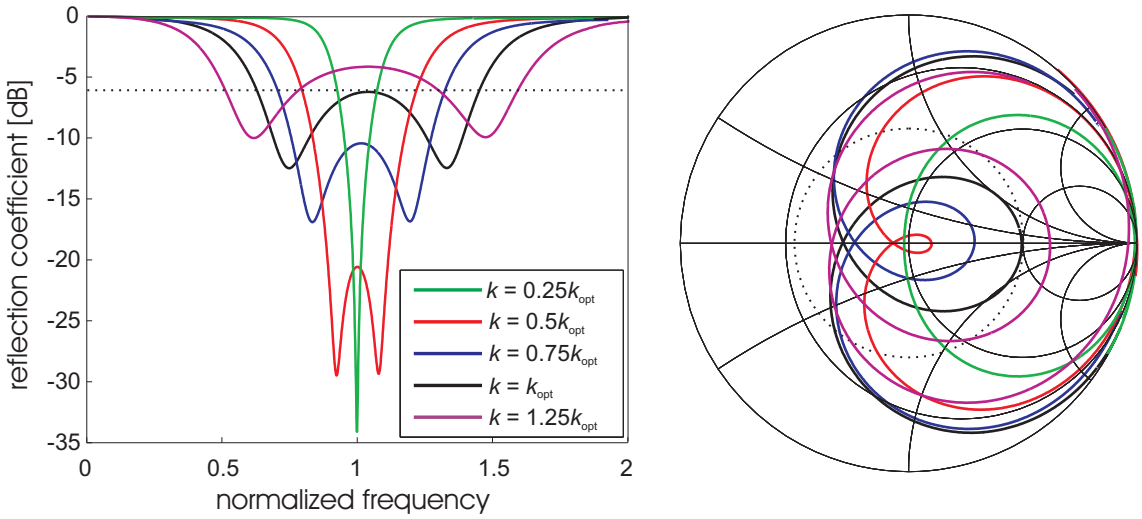

Figure 3.6: Effect of the coupling k between the coupling element and the chassis resonator. Chassis resonant frequency f_{rc} is normalized to 1.

As can be noticed in Figure 3.6, the largest 6 dB return loss bandwidth is achieved with optimal coupling factor k_{opt}. If the coupling k is smaller than the optimal value, the 'inner loop' on the Smith chart is smaller and the achievable 6 dB bandwidth is also clearly lower. On the other hand, if the coupling k becomes larger than the optimal value, the inner loop becomes too large to fit inside the 6 dB return loss circle on the Smith chart. Similar results was reported with two coupled patch antennas in [12].

The effect of the difference between the center frequency f_m of antenna and the resonant frequency f_{rc} of the chassis wavemode is presented in Figure 3.7. The optimal operation (largest bandwidth) is achieved when the resonant frequencies are equal, i.e. $f_m = f_{rc}$, in which case the inner loop circulates the center of the Smith chart symmetrically. From the bandwidth point of view it is advantageous to tune the chassis wavemode frequency to match as well as possible with the center frequency of the antenna.

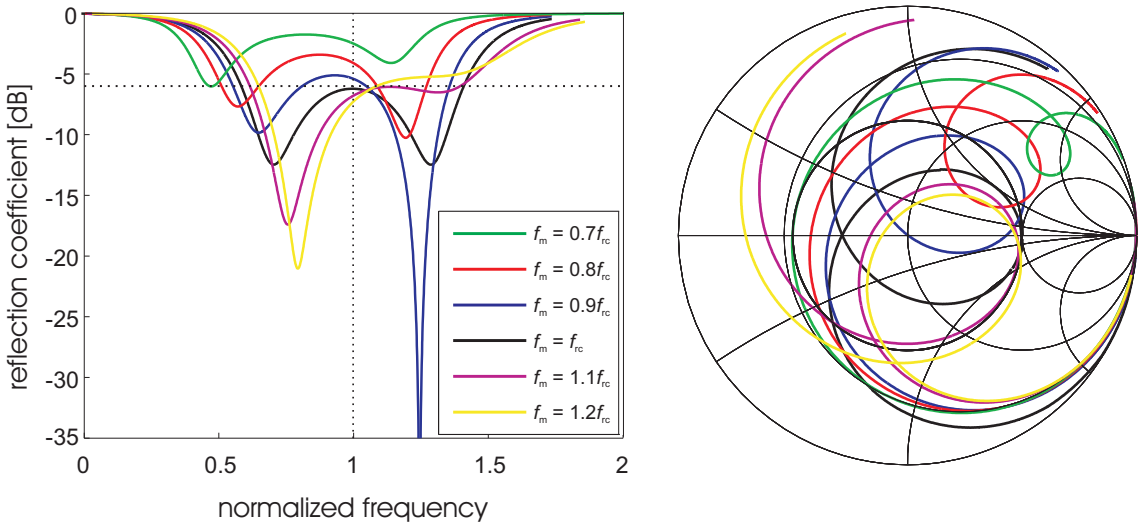

Figure 3.7: Effect of the difference between the resonant frequency f_m of the antenna and the resonant frequency f_{rc} of the chassis.

3.4 Capacitive coupling element antennas

This section will present capacitive coupling elements in detail. Figure 3.8 presents a capacitive coupling element structure without the matching circuitry and its simulated reflection coefficient.

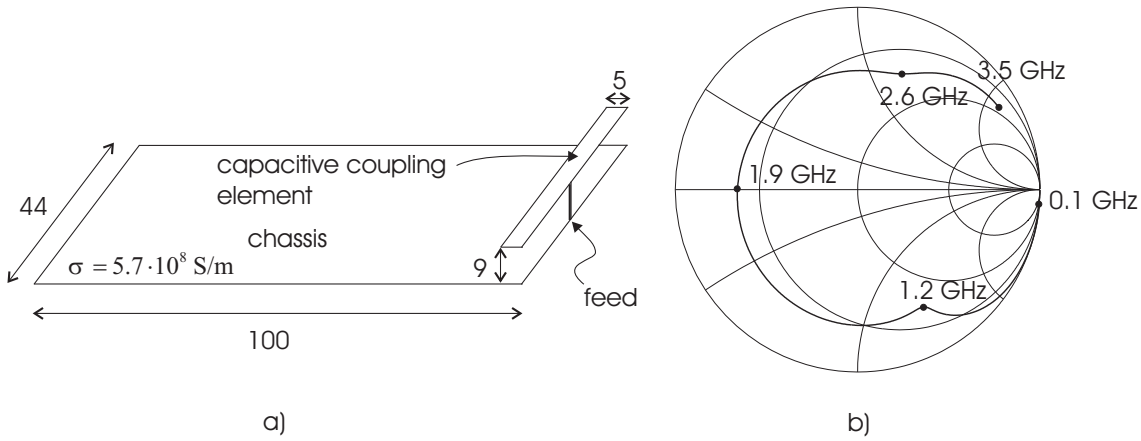

Figure 3.8: a) Capacitive coupling element structure (without the matching circuitry) and b) its reflection coefficient as a function of frequency on the Smith chart.

The structure is called capacitive because the coupling is implemented (mainly) via electric fields (see Figure 3.4a) and thus, the reflection coefficient, or impedance, is on the capacitive half of the Smith chart at lower UHF frequencies, see Figure 3.8.

The lowest order wavemode of the chassis can be estimated using (3.4): $f_{rc} \approx$ 1.1...1.2 GHz when $l = 100$ mm. Thus, a small rise can be noticed at 1.2 GHz in the impedance curve in Figure 3.8.

As can be seen in Figure 3.8, the antenna is not matched to 50 Ω at any frequency and thus in practice a matching circuitry is needed. Each simulated impedance point can be critically matched with an L-section matching circuit using the methods presented in Chapter 2, see Figures 2.1 and 2.2. The matching circuit design procedure was automatized with a Matlab code[2]. The reflection coefficients were calculated for each matching point and from those the achievable 6 dB return loss bandwidths were determined, see Figure 3.9.

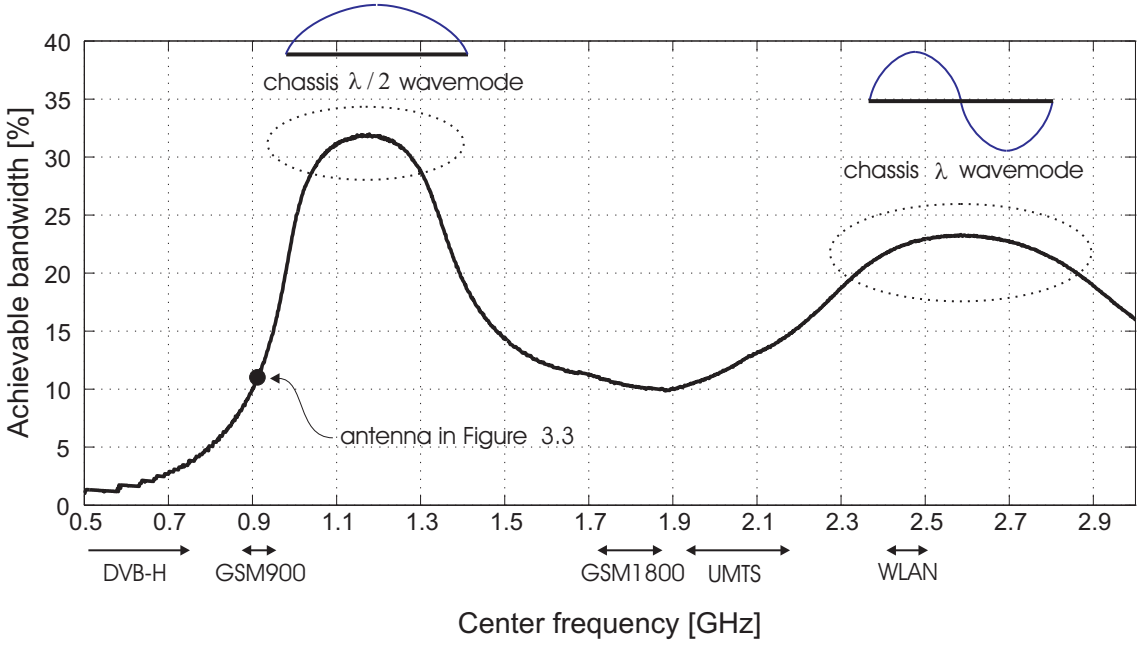

Figure 3.9: Achievable 6 dB return loss bandwidths as a function of the matching center frequency.

Certain bandwidth maxima can be noticed in the curves in Figure 3.9. Those maxima happen at the half and full wavemode resonant frequencies (here at 1.2 and 2.6 GHz) of the chassis. Since those are determined by the length of the chassis, it has significant influence on the bandwidth achieved with the antenna. By lengthening the chassis the bandwidth maxima moves to lower frequencies. Hence, the optimal

[2]The Matlab code was programmed by Dr. Juha Villanen at the Radio Laboratory of Helsinki University of Technology.

chassis length depends on the frequency band used. For example, at the center frequency of DVB-H, 610 MHz, the optimal chassis length is about 190 mm, see (3.4). Nevertheless, the length of modern monoblock mobile terminals is much shorter, see Figure 1.1, and because of that, the length of the chassis cannot be optimally chosen from the (DVB-H) antenna operation point of view. Fortunately, there are also other ways to optimize the antenna operation.

3.4.1 Optimization of coupling elements

Since the rise in the reflection coefficient caused by the chassis lowest order wavemode at 1.2 GHz in Figure 3.8b is not very large, the coupling between the capacitive coupling element and the chassis wavemode is rather small. Anyway, sufficient bandwidths could be achieved e.g. for GSM900, GSM1800, UMTS, and WLAN/Bluetooth systems. On the other hand, at lower frequencies, especially at the DVB-H frequencies, the achievable 6 dB return loss bandwidth is only few per cent and thus further optimization of the capacitive coupling element is needed.

By strengthening the coupling between the coupling element and the chassis wavemode, larger bandwidth can be achieved [22], [23]. The strongest possible coupling is gained by placing the coupling element to the maximum of the electric fields[3] and directing the surface of the element perpendicularly to the electric fields of the dominant wavemode of the chassis [22]. For a dipole-type structure, like the chassis, the strongest electric fields are located on the shorter ends of the chassis. For the strongest possible coupling, the coupling element needs to be placed beyond the edge of the chassis[4]. Furthermore, the element can be bent over the shorter edge of the chassis. In Figure 3.10 the achievable bandwidths of two different coupling elements are compared with the achievable bandwidth of the coupling element presented in Figure 3.8.

[3]The most commonly used internal antennas in mobile terminals, PIFA and IFA, do not couple optimally since the electric fields near the short pin are weak and due to that the coupling is reduced.

[4]If the length of the structure is held constant, the metallization must be removed below the element.

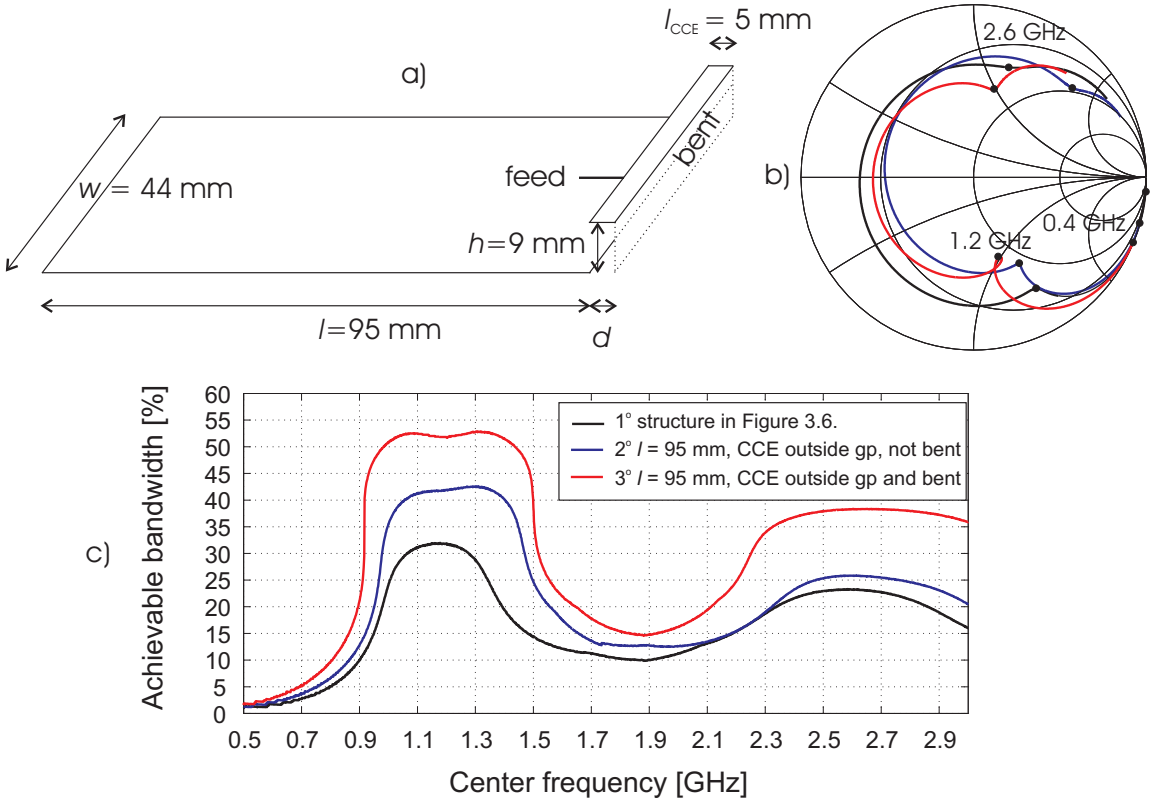

Figure 3.10: a) Different capacitive coupling element structures without the matching circuits and b) their impedances on the Smith chart. c) Achievable 6 dB return loss bandwidths as a function of the matching center frequency.

As can be seen in Figure 3.10, the optimization of the place and shape of the coupling element is a very efficient way to increase the achievable bandwidth. Since the coupling becomes larger, the rise in the reflection coefficient at 1.2 GHz in Figure 3.10b can be noticed to become larger, too. In [2] it was shown that the strongest coupling (and consequently the largest bandwidth) is achieved if the coupling element is totally outside the chassis, i.e. $d = l_{CCE}$ in Figure 3.10. Further increase in the bandwidth can be done by increasing the volume occupied by the coupling element, i.e. increasing d and/or h (see Figure 3.10a).

When the coupling to the dominant wavemode becomes larger, the electric fields near the coupling element (and in the talk position consequently also in the user's head) become larger too and thus, the specific absorbtion rate (SAR) values caused by the structure increase [19], [22]. The type of the antenna element is not significant for the SAR since the same increase in the SAR is discovered also e.g. with PIFA

and monopole antennas [19]. Definite drawback of the increased coupling is the increase in the SAR[5] and the decrease in the radiation efficiency at the same time [19], [22]. The SAR characteristics of coupling element antennas have also been examined in [25], [26] and [27]. As explained, the achievable bandwidth and SAR behave contrarily. Thus, the antenna designer needs to find the optimal coupling in order to meet the bandwidth and SAR requirements. Fortunately, it is relatively easy to control the coupling by optimizing the place, shape and volume of the coupling element.

3.4.2 Modifying chassis shape

As presented earlier, the lowest order wavemode of the typical-size chassis does not usually coincidence with the operation frequencies of the current communication systems. The electrical length of the chassis can be increased without increasing the physical length by introducing a slot in the chassis, see Figure 3.11.

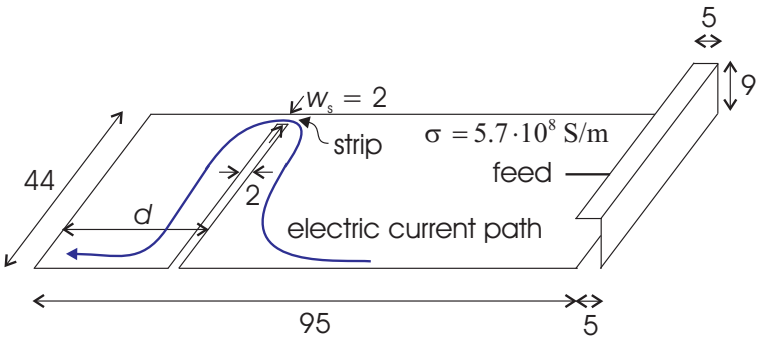

Figure 3.11: Effect of the slot on the electric current path.

The slot lengthens the electric current path on the chassis and thus, the resonant frequency of the chassis wavemode decreases [19]. This is especially important for the systems operating below 1.2 GHz, i.e. DVB-H and GSM850/900, but it also affects the performance of other systems since it changes the λ wavemode. The resonant frequencies of the $\lambda/2$ wavemode are simulated with IE3D as a function of

[5]Since DVB-H is only receiving, SAR values are irrelevant. However, transmitting systems, such as GSM900 etc, are also included in the same terminal and thus, SAR values of the whole radiation system are very important.

the distance d of the slot from one end of the chassis, see Figure 3.12.

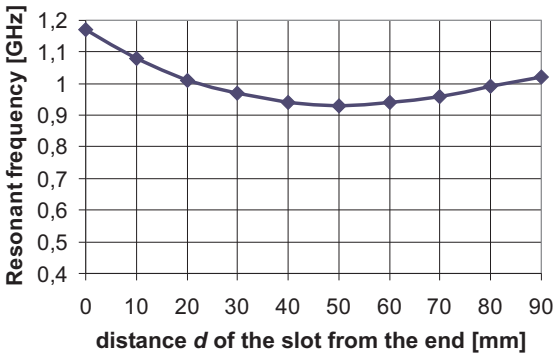

Figure 3.12: Resonant frequency of the chassis as a function of the distance d of the slot from one end. $d = 0$ mm means that there is no slot.

As can be seen in Figure 3.12 the resonant frequency of the chassis can be decreased as much as 20.5% if the slot is placed in the middle of the chassis. The most optimal place of the slot occurs there because in the dipole-type current distribution the current maximum is also in the middle and the effect of the slot is then the largest possible. The resonant frequency of the chassis can be further decreased by narrowing the width of the strip, or by introducing additional slots.

According to IE3D simulations (not presented here), the use of slots is problematic if there are conductive objects, such as a screen, battery, data or DC lines, on top of the slot because the conductive objects short circuit the slot and the effect of the slot is impaired. Thus, to guarantee best possible effect of the slot, the location of the slot has to be chosen by taking into account the placing of other objects. The data and DC lines can be placed e.g. on top of the strip. The data could also be transferred across the slot using optical link, see Figure 3.13. Also here, the SAR values of the transmitting antennas need to be checked since the slot may affect an increase in SAR compared to solid chassis.

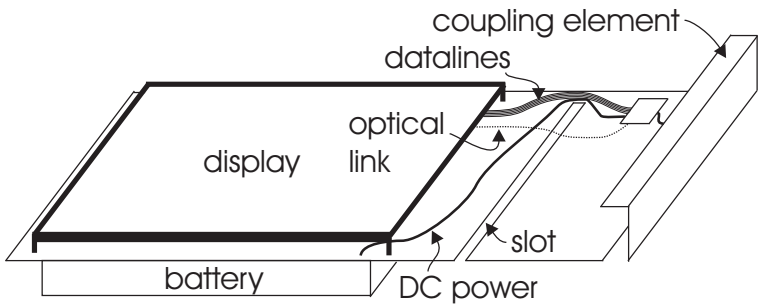

Figure 3.13: Recommended location of the slot chosen according to the placing of other conductive objects such as screen and battery.

3.5 Direct feed

By introducing direct feed antennas the currents can be coupled galvanically to the surface of the chassis. This way the coupling to the chassis wavemode becomes relatively strong as well as the volume occupied by the 'antenna' decreases fairly much. The feed has to be implemented over an impedance discontinuity that can be formed e.g. by a slot, see Figure 3.14. Anyway, obviously for the EMC issues, the ground plane of a mobile terminal needs to be one solid piece of metal and due to that the strip is needed to connect the segmented parts. The operation of such direct feed antennas are demostrated e.g. in [28], [29] and [30].

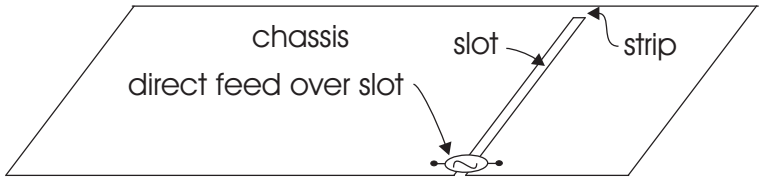

Figure 3.14: Principle of the direct feed.

Since the height of the direct feed antenna is very low, the antenna suits very well for low profile mobile terminals[6]. Herein, no conductive objects should be place on the top of the slot. The resonant frequency of the chassis can furthermore be decreased using another slot, see Figure 3.15.

The direct feed suits particularly well for terminals which naturally contains a slot. For example in a clamshell phone there is a natural slot between the lower and upper

[6]The SAR values of the antenna are not verified here.

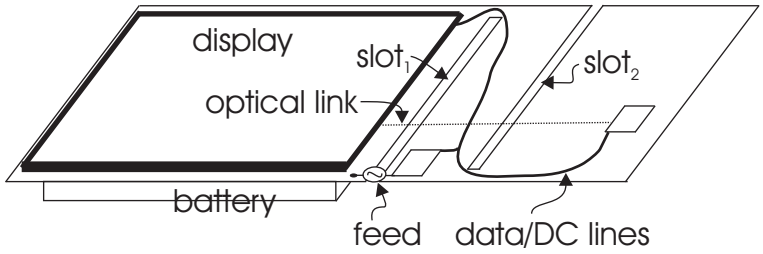

Figure 3.15: Direct feed antenna in a low profile terminal.

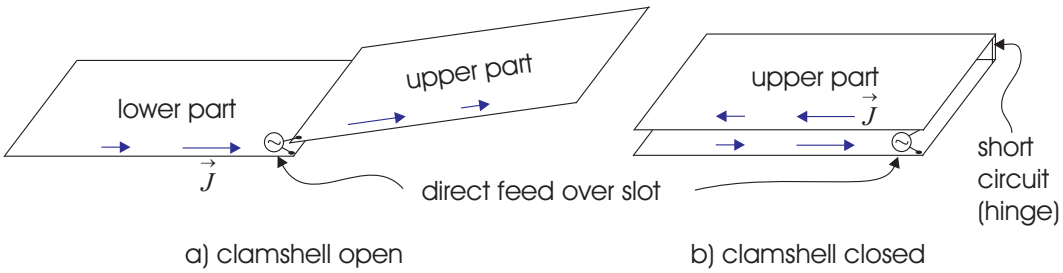

Figure 3.16: Direct feed applied for a clamshell terminal.

parts and thus, the antenna can be fed across the slot, see Figure 3.16a. Benefit of this structure is that the volume occupied by the antenna is very small, almost zero. Therefore, one can refer the direct feed antenna also as a 'zero volume antenna'. When the clamshell is open, the length of the terminal (and consequently the length of the chassis too) is longer compared to the typical length of a traditional monoblock terminal. Thus, the lowest order wavemode of the clamshell terminal chassis occurs at the frequency clearly lower than that of traditional monoblock terminals [21]. As discussed earlier, this is a benefit for the systems operating at lower UHF frequencies. The drawback of the antenna arises when the clamshell is closed; the operation of the antenna is apparently challenging since the electric fields induced by the currents of the $\lambda/2$ wavemode in the lower and upper parts partly cancel each other in the far field [24], see Figure 3.16b.

3.5.1 Matching of direct feed antennas

The direct feed structure in Figure 3.17a is simulated with IE3D and the impedances are shown on the Smith chart in Figure 3.17b.

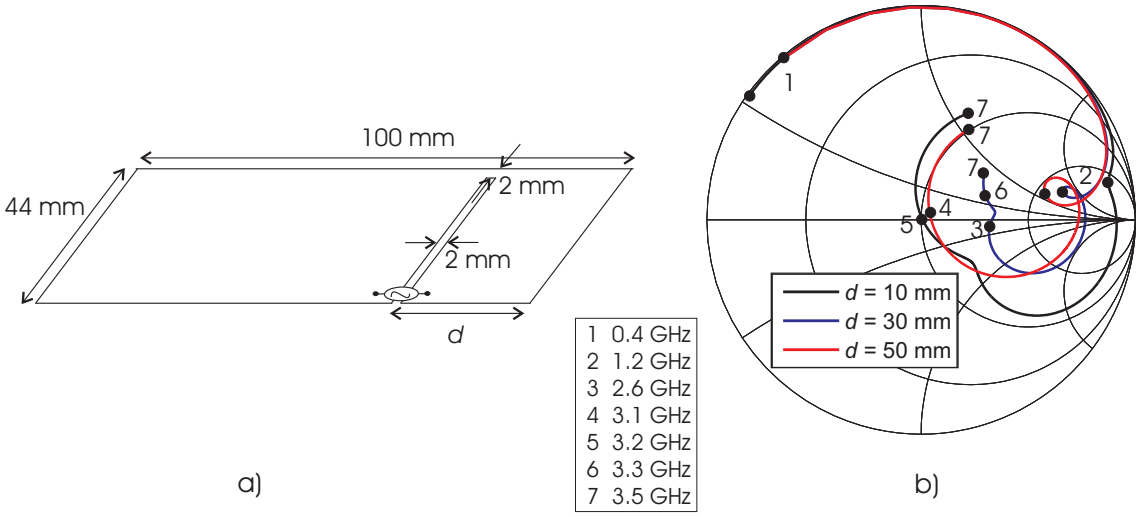

Figure 3.17: a) Direct feed structure simulated. b) The impedance curve on the Smith chart with different slot locations.

Each impedance point in Figure 3.17b can be matched with an L-section matching circuit using the methods presented in Chapter 2. As an example the antenna structure is matched at 1.2 GHz (at the resonant frequency of the chassis lowest order wavemode) and the reflection coefficients are shown in Figure 3.18. The results including the matching circuit component values are reported in Table 3.1. As can be seen from the Smith chart presentation, the dual-resonant operation is not optimal because the inner loop around the center of the Smith chart is too small, i.e. the coupling (factor k) is not large enough, see Figure 3.6 and [12].

Table 3.1: Achievable 6 dB return loss (RL) bandwidths and the matching circuit component values for direct feed antennas.

d [mm]	6 dB RL band [MHz]	BW [MHz]	B_r [%]	L [nH]	C [pF]
10	1099 - 1347	248	20	47	0.67
30	979 - 1559	579	46	22	1.35
50	947 - 1654	707	54	21	1.50

According to Figure 3.18a and Table 3.1 the largest bandwidth is achieved when the feeding slot is in the middle of the chassis. Since the current maximum of the lowest order wavemode is also located in the middle, it is obvious that the largest coupling is also reached there. Consistently with the capacitive coupling element antennas, the largest bandwidth is achieved when the coupling to the chassis wavemode is the

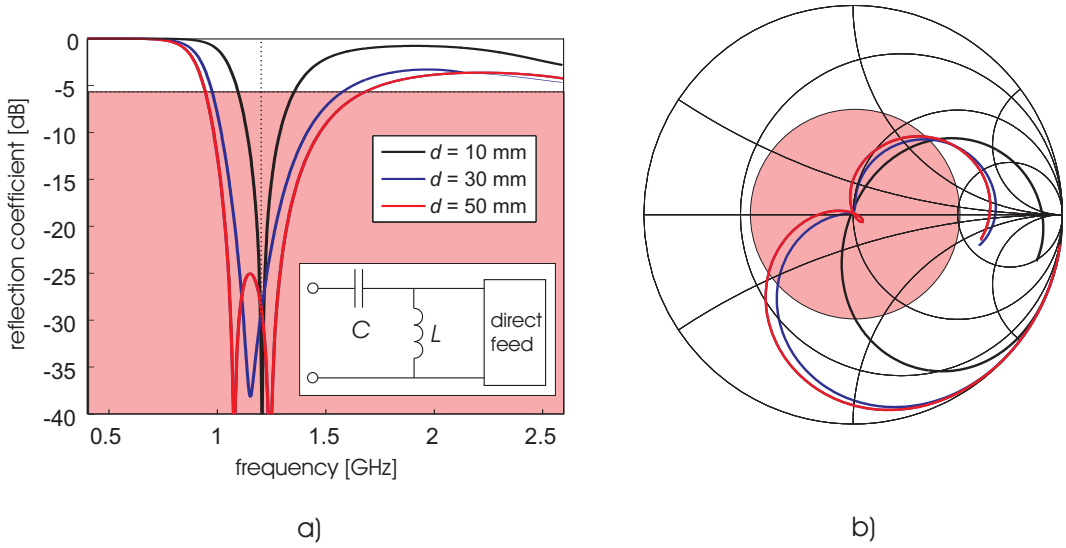

Figure 3.18: Reflection coefficient of the direct feed antennas with different d a) in the Cartesian coordinate system and b) on the Smith chart. The antenna is matched at 1.2 GHz.

strongest possible. The coupling between the feed and the chassis wavemode can also be controlled with the length of the feeding slot. According to IE3D simulations (not presented here), the longer the slot is, i.e. the narrower the strip is, the stronger the coupling becomes. The strongest coupling would be achieved with total cut, i.e. no strip. In that case the antenna would work as a thick center-fed dipole antenna.

When comparing the achievable bandwidths between the capacitive coupling element (Figure 3.10c) and direct feed antennas, one can notice the achievable bandwidths at 1.2 GHz are approximately equal. However, the profile of the direct feed antenna is very low compared to the capacitive coupling element antennas.

Next, the direct feed antenna in Figure 3.17a is matched at 0.9 GHz. The results are shown in Figure 3.19 and Table 3.2. One can also now notice from the Smith chart presentation that the antenna operation is not optimal (see Figure 3.7) since the matching frequency and the resonant frequency of the chassis are not equal ($f_m \neq f_{rc}$). According to Figure 3.19 and Table 3.2, broad bandwidth can be achieved when $d = 50$ mm[7] but in the other cases the bandwidth is significantly

[7]Antenna structure similar to this, designed and manufactured at the Radio Laboratory of TKK, won the ACE Small Antenna Contest 2007 in the 'Single band antenna' category. The total efficiency of the prototype antenna was better than 74% across 880 - 960 MHz [31].

smaller. Compared to 1.2 GHz the bandwidth is quite similar when $d = 50$ mm, but generally bandwidths are narrower because of moving away from the chassis wavemode frequency, but also because the antenna becomes smaller in wavelengths.

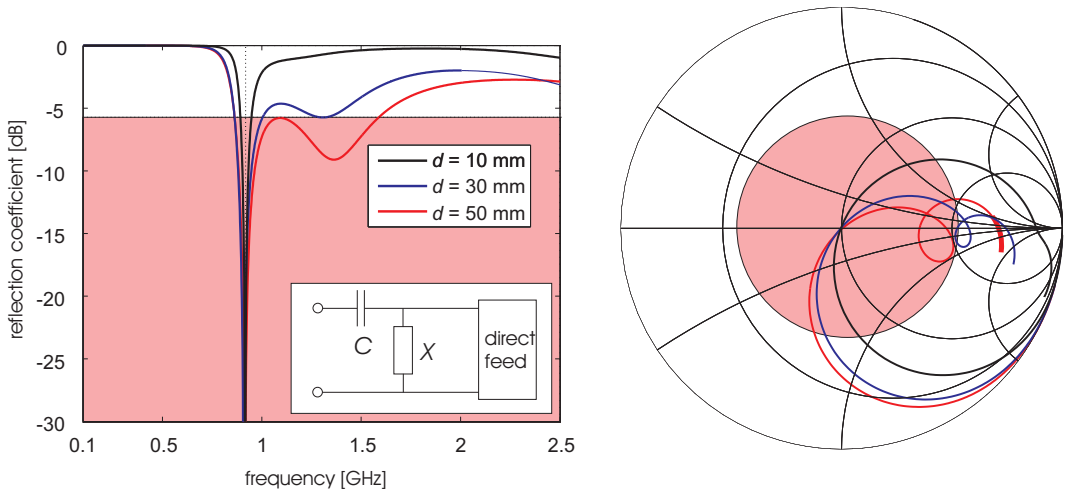

Figure 3.19: Reflection coefficient of the direct feed antennas with different d a) in the Cartesian coordinate system and b) on the Smith chart. The antenna is matched at 0.9 GHz.

Table 3.2: Achievable 6 dB return loss (RL) bandwidths and the matching circuit component values for direct feed antennas.

d [mm]	6 dB RL band [MHz]	BW [MHz]	B_r [%]	X	C [pF]
10	893 - 946	53	5.8	0.25 pF	0.474
30	864 - 996	132	14	120 nH	0.825
50	864 - 1571	707	58	63 nH	0.965

Chapter 4

Handheld DVB terminal antennas

This chapter presents several internal DVB-H antenna solutions for mobile terminals. In order to provide the reader with sufficient understanding of the proposed antenna solutions, requirements and design aspects for the DVB-H antennas will be reviewed first. After that, the implementation of DVB-H antennas based on compact coupling structures is examined and several prototypes and designs are presented. In the end of the chapter the user effect of DVB-H antennas and interoperability of DVB-H antennas with different transmitting antennas are studied.

4.1 Design aspects of DVB-H antennas

The wavelength at the center frequency (0.610 GHz) of the DVB-H band (470 - 750 MHz) is about 500 mm. As the length of a typical-size monoblock mobile terminal is about 110 mm (see Figure 1.1), a DVB-H antenna implemented inside a mobile terminal will be electrically small. Due to that, broadband operation is very challenging to implement with the typical matching criterion, 6 or 10 dB return loss.

Instead of having high performance in DVB-H antennas, the goal is to provide antenna performance which is only just enough for the operation with certain reliability level. Since DVB-H is receiving only, lower antenna performance can be accepted than in transceiver antennas. In small antennas reduced performance means re-

duced total efficiency. The ultimate requirement in the DVB-H receiving system is to reach a sufficient signal-to-noise ratio over the DVB-H band. In order to estimate the lowest required total efficiency of an DVB-H antenna, an equation is derived in [32]:

$$\eta_{tot,min} = \frac{4\pi P_{rec,min}\eta_0}{E_{inc}^2 c_0^2 D} f^2, \tag{4.1}$$

in which $P_{rec,min}$ is the sensitivity of a receiver, η_0 is the wave impedance 377 Ω, E_{inc} is the typical minimum electric field strength guaranteed by the broadcasting network, c_0 is the speed of light, D is the directivity of an antenna (about 2 dBi for small antennas [33]) and f is the frequency used. In [34] it has been reported that the minimum electric field strength in indoor reception is typically better than E_{inc} = 55 dBμV/m. According to [35], the sensitivity of a DVB-H receiver can be expected to be about $P_{rec,min}$ = -90 dBm. These approximated values yield that the minimum total efficiency required in a DVB-H antenna is in the order of -16 ... -12 dB over the DVB-H band (0.47 - 0.75 GHz). According to this estimation it is possible to sacrifice the total efficiency in order to increase the bandwidth and at the same time reach sufficient signal-to-noise ratio. From the antenna designer point of view the performance of a DVB-H antenna has to be a trade-off between the total efficiency and feasible size of the antenna.

4.1.1 Performance specification of internal DVB-H antennas

The expected antenna performance has been given in terms of realized gain[1] in [35] and [36]. The realized gain of a DVB-H antenna inside a mobile terminal is expected to be in the order of -10 dBi to -5 dBi over 470 - 862 MHz, see Figure 4.1. When DVB-H is used in a terminal that includes also GSM900 (the case considered in this work), the frequency band of DVB-H is limited up to 750 MHz [35], [36]. In the following the presented realized gain limit is considered as a performance specification for DVB-H antennas. In handsets also other parts as display, battery, plastic covers and possible filters in the input of the DVB-H antenna will introduce implementation losses. Thus, simplified prototype antennas presented in this work

[1] Realized gain G_r is gain reduced by the matching losses: $G_r = \eta_{tot} D$ [10].

should have a suitable margin to the realized gain specification.

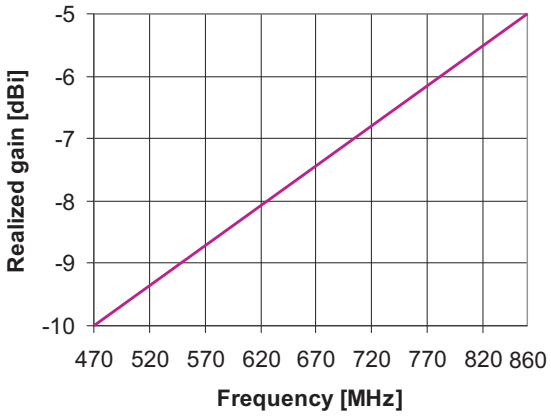

Figure 4.1: Expected realized gain G_r performance of a DVB-H antenna inside a mobile handset [35], [36].

4.1.2 Broadening bandwidth in DVB-H antennas

The design goal of an internal DVB-H antenna is to minimize the volume occupied by antenna element while the sufficient realized gain is achieved. Since the directivity of a small antenna is about 2 dBi [33] and it cannot be affected very much with the antenna design, the realized gain is mainly controlled by the total efficiency. An antenna can be matched (or coupled) in such a way that the bandwidth is significantly increased at the expense of lower total efficiency, see Figure 4.2.

Thus, the question is how much the total efficiency can be sacrificed in a DVB-H antenna and still meet the realized gain specification? As discussed in Chapter 2, accepting the mismatch will provide the highest possible total efficiency over a certain bandwidth. In this work, resistive losses are minimized and the total efficiency is sacrificed by accepting a certain mismatch. Since the DVB-H system is intended for reception only, higher mismatch level may be tolerated. On the other hand, as told earlier, there will certainly be implementation losses in a handset and their additional resistive load will improve matching but consequently decrease the total efficiency.

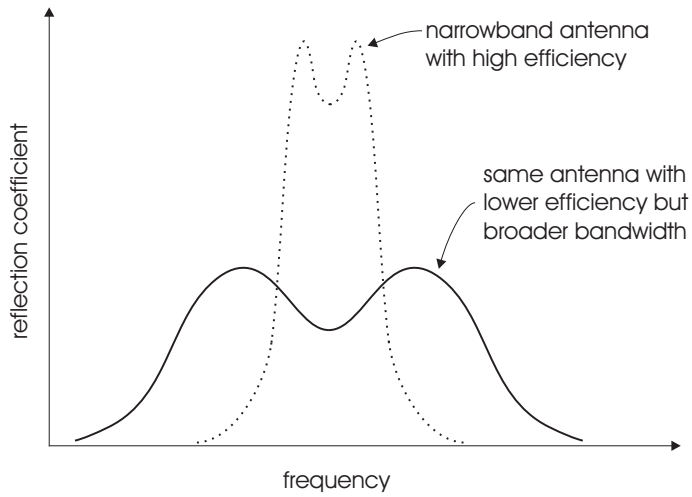

Figure 4.2: A narrowband antenna can be matched so that a larger bandwidth is covered with a lower total efficiency.

In [2] it was shown that in a lossless case the matching of 1.5 dB return loss yields a realized gain of approximately -3 dBi. Since the realized gain specification is between -10 and -6 dBi over the DVB-H band, the margin to the specification is at least about 3 dB. In this work this is considered to be a sufficient margin to the specification and thus in the following 1.5 dB return loss is used as the matching criterion for internal DVB-H antenna designs and prototypes.

4.2 Classification of DVB-H antennas and some implementation examples

DVB-H antennas can be divided into different categories according to their characteristics. The first division is between external and internal antennas, see Figure 4.3. External antennas are usually some kind of monopole structures like whip or helix antennas. Furthermore, antennas can be categorized as tunable and non-tunable antennas. Tunable antennas create an instantaneous resonance at a suitable frequency so that the wanted single DVB-H channel (frequency band) is covered. When the channel is changed, the resonant frequency of the antenna needs to be changed, too, see Figure 4.4a. Non-tunable antennas have time-invariant matching covering the whole frequency band, see Figure 4.4b.

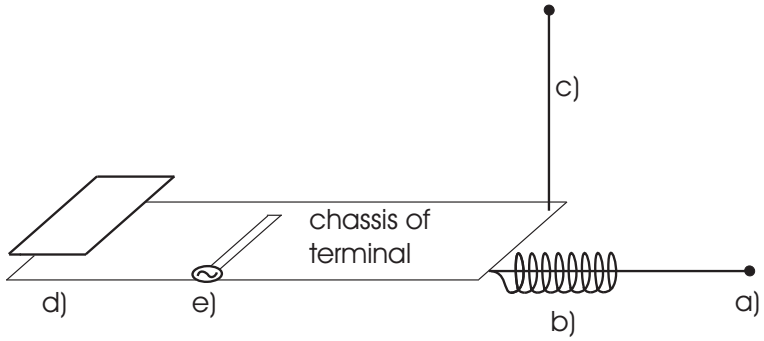

Figure 4.3: Possible DVB-H antennas. a), b) and c) are external antennas and d) and e) are internal antennas as shown in Chapter 3.

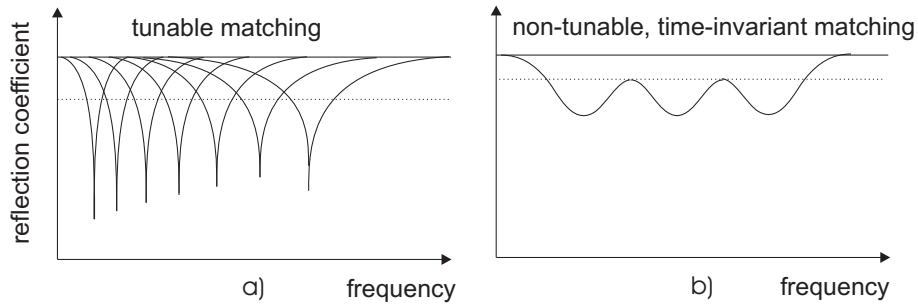

Figure 4.4: Typical frequency responses of the reflection coefficient of a) tunable antenna and b) non-tunable antenna.

4.2.1 Example antenna solution

A commercial DVB-H antenna is designed and manufactured by Pulse Finland Oy (part number W3520) [37]. The dimensions of the external antenna are 50.5 mm x 10.5 mm x 3.0 mm [length x width x thickness], the total volume being 1.6 cm^3. The antenna performance has been evaluated by the manufacturer on a test board whose dimensions are 100 mm x 45 mm [length x width]. In the using position the orientation of the antenna is perpendicular to the test board. The return loss over the DVB-H band (470 - 750 MHz) is approximately 3 dB. The margin to the realized gain specification is at least 4 dB. The main advantages of this antenna are good realized gain performance compared to the specification, and a rather simple antenna structure. A drawback is that it is external because users prefer internal antennas and they are also mechanically challenging to implement since they are more exposed to mechanical stress during use.

4.2.2 Tunable antennas

Tunable antennas are useful when the terminal and antenna are so small that the coverage of the whole bandwidth is challenging, such as in the case of DVB-H antennas. The simplest idea for tuning an antenna is to use electrically adjustable components, such as varactors. The capacitance of a varactor diode can be adjusted by the reverse DC bias over the component. An electrically adjustable inductor is more difficult to implement.

A varactor-tuned DVB-H antennas are introduced in [38], [39] and [40]. The antenna elements used are PIFA [38], capacitive coupling element [39] and monopole [40]. Advantages of these antennas are good matching and fairly compact antenna element size. Drawback of the antennas is the non-linearity of the varactor that will cause radiating interference components when GSM900 is used in the same terminal.

4.3 Capacitive coupling element based DVB-H antennas

This section introduces the implementation of DVB-H antennas based on the capacitive coupling elements which were presented in Section 3.4.

4.3.1 Prototype antenna

One of the first internal DVB-H antennas published is based on the capacitive coupling element [2]. The antenna is intended for a tablet-size mobile terminal, the chassis dimensions being 130 mm x 75 mm [length x width]. The most optimal location and shape of the coupling element were studied by IE3D simulations [2]. The dimensions of the element are 5 mm x 75 mm x 4 mm [length x width x height] and thus the total volume occupied by the element is only 1.5 cm^3, see Figure 4.5. A manufactured prototype was presented in [41].

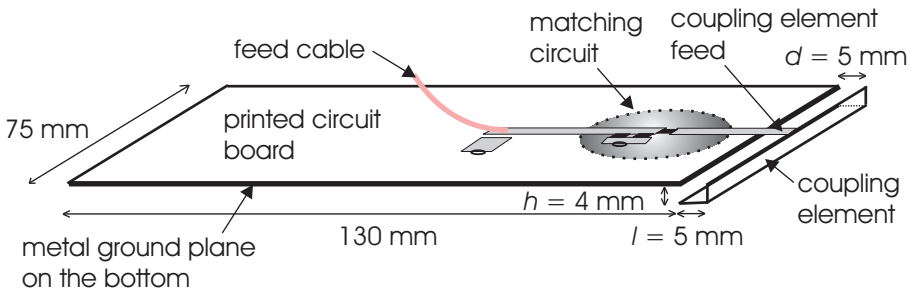

Figure 4.5: Capacitive coupling element based DVB-H antenna.

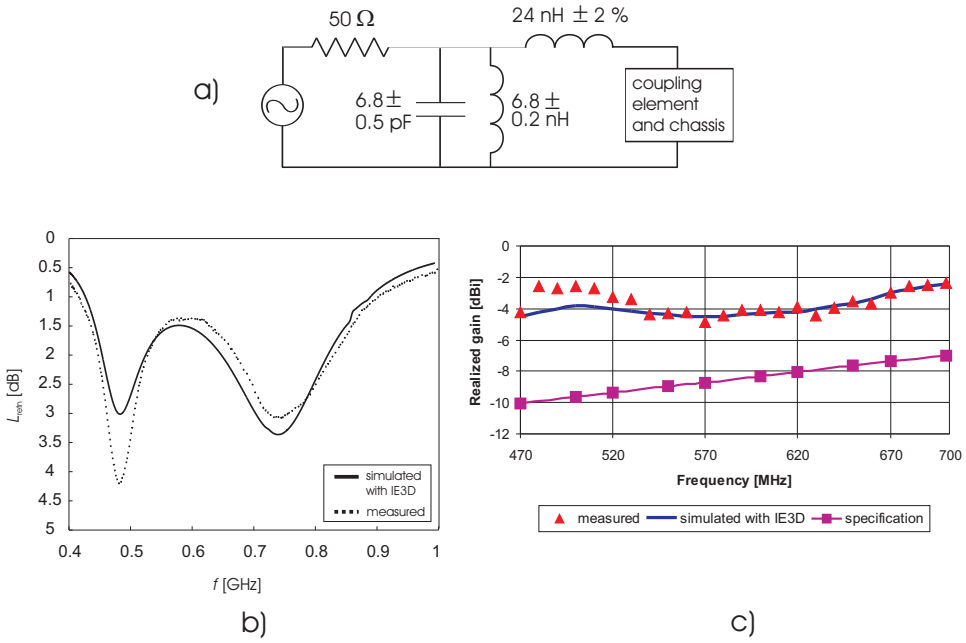

Figure 4.6: a) Dual-resonant matching circuit, b) simulated and measured reflection coefficients, c) simulated and measured realized gain [41].

The matching is implemented with a dual-resonant lumped-element matching circuit, which is presented in Figure 4.6a. The simulated and measured frequency responses of the reflection coefficient of the prototype are shown in Figure 4.6b. The return loss is at least about 1.5 dB over the DVB-H band. The difference between the simulated and measured results is mainly caused by the relatively large tolerance in the matching circuit chip capacitor ($C = 6.8 \pm 0.5$ pF). The simulated and measured realized gain is shown in Figure 4.6c and the realized gain specification is fulfilled with a 4 dB margin across the DVB-H band 0.47 - 0.702 GHz[2]. The

[2]The prototype was manufactured in 2005 when the DVB-H band was limited to 0.702 GHz if GSM900 was used in the same terminal

radiation pattern is similar to that of a dipole antenna and the maximum directivity is about 2 dBi.

4.3.2 Commercial solutions

The commercial DVB-H antenna designed and manufactured by Pulse Finland Oy (part number W3510) is also based on the capacitive coupling element [37], see Figure 4.7a. The dimensions of the coupling element are 6.6 mm x 45 mm x 5 mm [length x width x height] and thus the total volume occupied by the coupling element is only 1.5 cm^3. According to the datasheet in [37], the antenna has been evaluated by the manufacturer on a metallic test board whose size is 100 mm x 45 mm [length x width]. The margin to the realized gain specification is less than 1 dB. Instead of placing the matching circuitry on the printed circuit board, like in Figure 4.5, it is placed on the side of the coupling element, see Figure 4.7a.

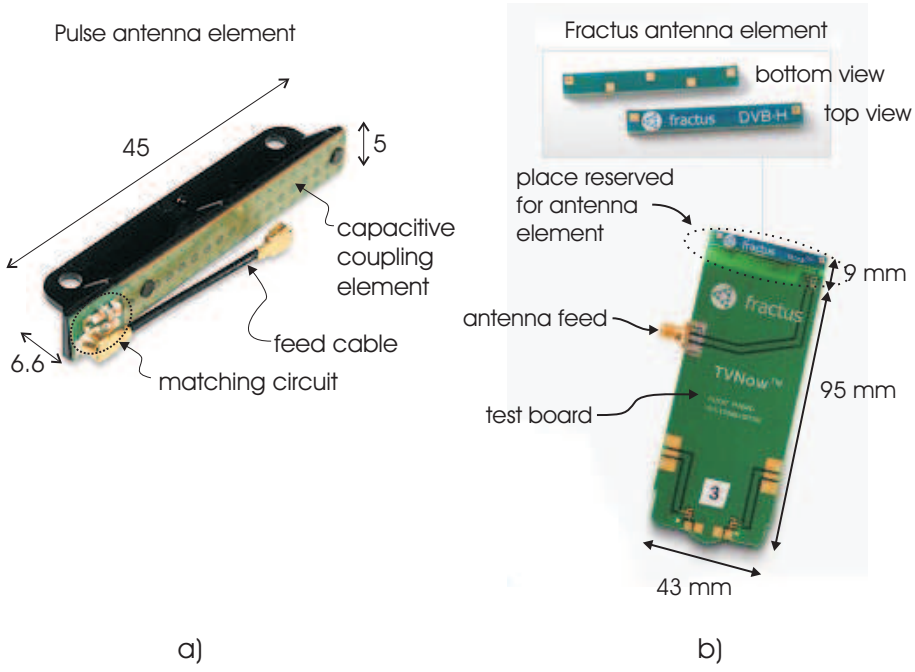

Figure 4.7: a) Capacitive coupling element based DVB-H antenna by Pulse Finland (metallic test board not shown) [37] and b) internal DVB-H antenna by Fractus [42].

A commercial DVB-H antenna manufactured by Fractus [42] is apparently based on some kind of capacitive coupling element, see Figure 4.7b. The antenna element itself is very compact in size, the dimensions are 4.8 mm x 40 mm x 5 mm [length

x width x height] and thus, the volume occupied is only 0.96 cm^3. The effective volume occupied by the element inside a mobile terminal is anyway more, 2.6 cm^3, because free space around the antenna element has to be left, see Figure 4.7b. The chassis dimensions are 95 mm x 43 mm [length x width] and the matching is implemented with a multi-resonant lumped element matching circuitry. The margin to the realized gain specification is less than 1 dB.

4.3.3 Coupling element dimensions versus terminal size

Table 4.1 summarizes the performance and size characteristics of the presented capacitive coupling element based antennas. The antenna prototype in Figure 4.5 is called TKK antenna.

Table 4.1: Summary of the presented capacitive coupling element based DVB-H antennas.

case	element volume [cm^3]	chassis size [mm x mm]	minimum return loss R_{retn} [dB]	margin to G_r specs [dB]
TKK	1.5	130 x 75	1.5	4
Pulse	1.5	100 x 45	-	< 1
Fractus	2.6	95 x 43	-	< 1

The TKK prototype has sufficient margin to the realized gain specification but the size of the chassis is too large for today's typical-size handsets, like N77 in Figure 1.1. The commercial antennas manufactured by Pulse and Fractus would be suitable in size for typical-size terminals but the margin to the realized gain specification may not be adequate to meet the expected realized gain inside real handsets. Hence, there is a motivation to study the smallest possible volume of coupling element antenna structure, which has both the chassis dimensions of today's handsets and a sufficient margin to the realized gain specification.

In the following, the minimum height of the coupling element with given terminal outer dimensions and shape will be studied. Five different dimensions of a terminal are used, three of them for a monoblock terminal, one for a tablet and one for an open clamshell terminal, see Table 4.2. The height h of the terminal is one variable.

The terminal outer dimensions, illustrated in Figure 4.8, are supposed to enclose the chassis, antenna element and other relevant components of the handset.

Table 4.2: Terminal dimensions.

terminal name	dimensions [mm x mm]
small monoblock	100 x 44
typical monoblock	110 x 48
large monoblock	120 x 52
tablet	135 x 75
open clamshell	165 x 40

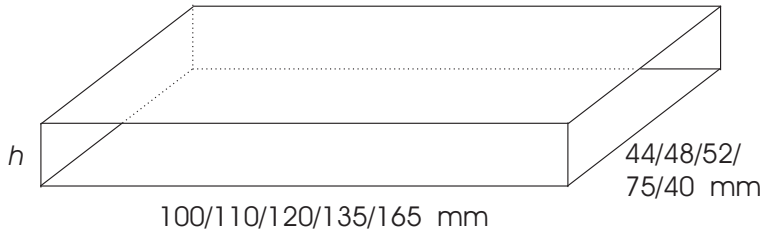

Figure 4.8: Outer dimensions of the terminals.

The length l_{CCE} of the coupling element is 5 mm in all cases and thus the length of the chassis is 5 mm shorter than the total structure length. The shape and location of the coupling element are optimized to produce the strongest possible coupling (see Section 3.4.) and consequently the largest bandwidth, see Figure 4.9.

The study is made as follows. The reflection coefficient of the antenna structure is simulated with IE3D and a suitable matching circuit is designed using AWR APLAC circuit simulator [43]. The minimum height h of the coupling element giving the return loss of 1.5 dB[3] across the DVB-H band 470 - 750 MHz is determined. Three different cases are studied for each terminal size: First and second are dual-resonant and triple-resonant matching, respectively, when the chassis is solid, i.e. no slot. The third case is triple-resonant matching and a 2 mm wide slot introduced in the middle of the chassis. The matching circuit topologies are shown in Figure 4.9. In the open

[3] As presented earlier in this chapter, 1.5 dB return loss leads to the realized gain in the order of -3 dB for a lossless antenna, i.e. at least 3 dB above the specification

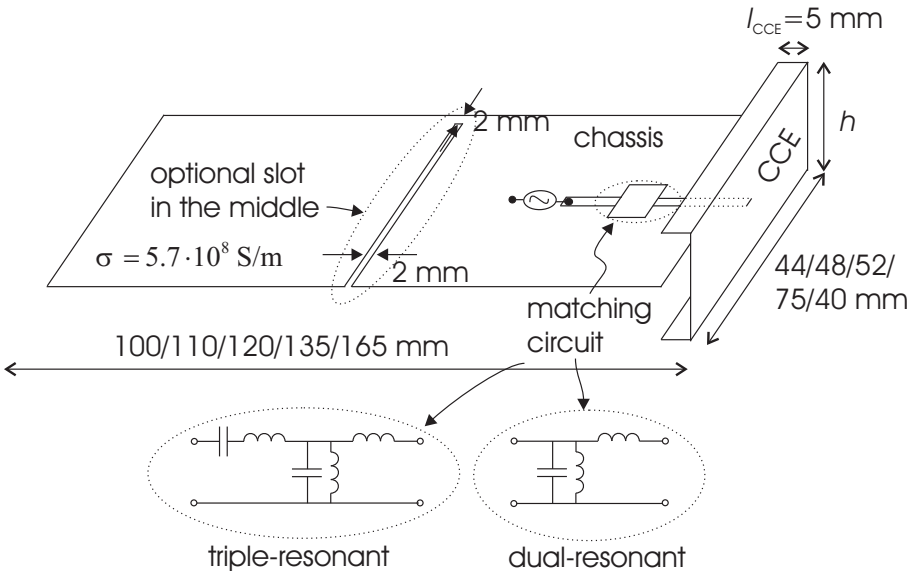

Figure 4.9: Capacitive coupling element based DVB-H antenna attached to the one end of the terminal.

monoblock case the slot is in the middle in all cases. The minimum heights are shown in Figure 4.10. The volume [cm^3] occupied by the coupling element in different cases are reported in Table 4.3. The study was conducted with ideal matching circuit components. In practice the losses and the variation of the component values will affect the performance.

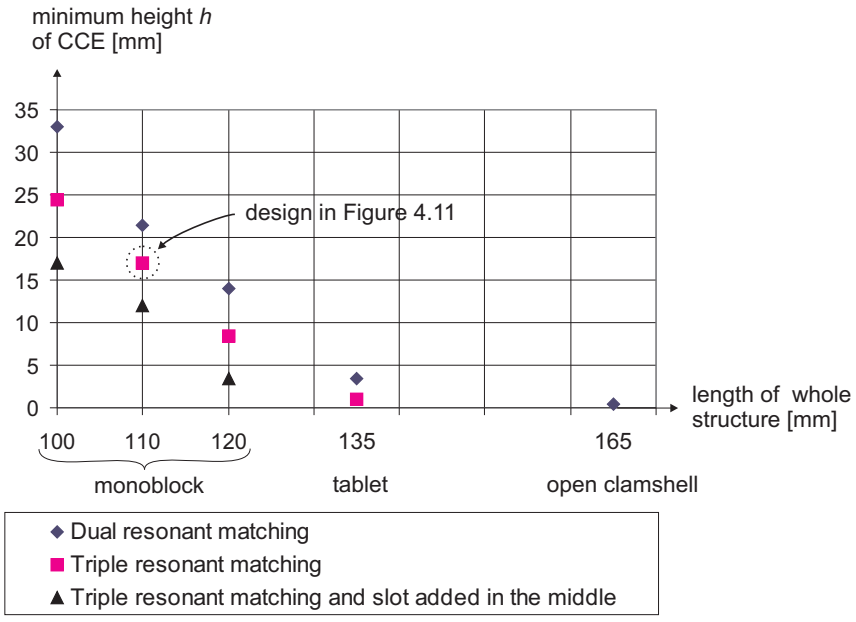

Figure 4.10: Effect of different terminal sizes and shapes on the minimum coupling element height with dual-resonant and triple-resonant matching.

Table 4.3: The volume [cm^3] occupied by the coupling element in each cases.

terminal name	dual-resonant matching	triple-resonant matching	triple-resonant matching and slot
small monoblock	7.3	5.3	3.7
typical monoblock	5.3	4.1	2.9
large monoblock	3.6	2.1	0.78
tablet	1.5	0.56	-
open clamshell	0.38	-	-

Based on the results in Figure 4.10 and Table 4.3, the size of the chassis has generally very significant effect on the minimum height of the element. While very big coupling elements compared to the commercial antennas are needed to reach the sufficient margin with rather short monoblock terminals, the tablet-size terminal can allow rather small coupling element. The minimum height of the tablet-size terminal is in good agreement with the height of the TKK prototype in Figure 4.5. The open clamshell-size terminal can have a very thin coupling element. Triple-resonant matching instead of dual-resonant matching is shown to decrease the minimum height of the coupling element very effectively. A slot in the middle of the chassis also allows using clearly smaller coupling elements. Lastly, the study indicates that it is difficult to fulfil the realized gain specification with a small coupling element (e.g. 2 cm^3) inside typical-size monoblock terminals.

4.3.4 Simulated design for typical-size terminal

The purpose of this subsection is to demonstrate a DVB-H antenna design for a typical-size terminal. The minimum height of the coupling element for a typical size monoblock with triple-resonant matching is 17 mm, see Figure 4.10. That design is considered to be a good compromise between the size of the coupling element and a sufficient performance. The antenna structure and lumped element matching circuit (ideal components) are shown in Figure 4.11. The simulated reflection coefficient is shown in Figure 4.12 and the simulated realized gain is shown in Figure 4.13.

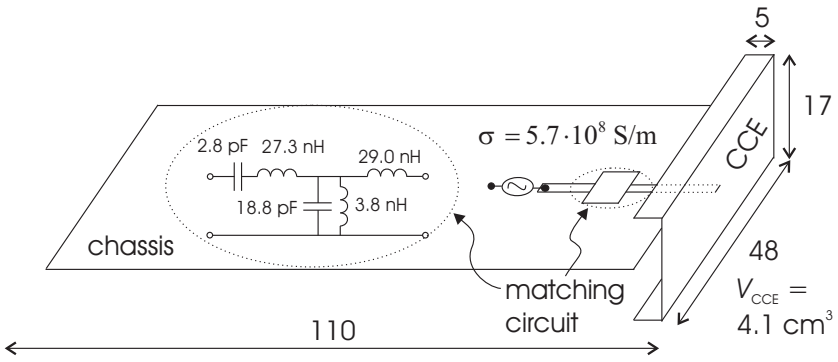

Figure 4.11: Simulated DVB-H antenna design for N77-size terminal.

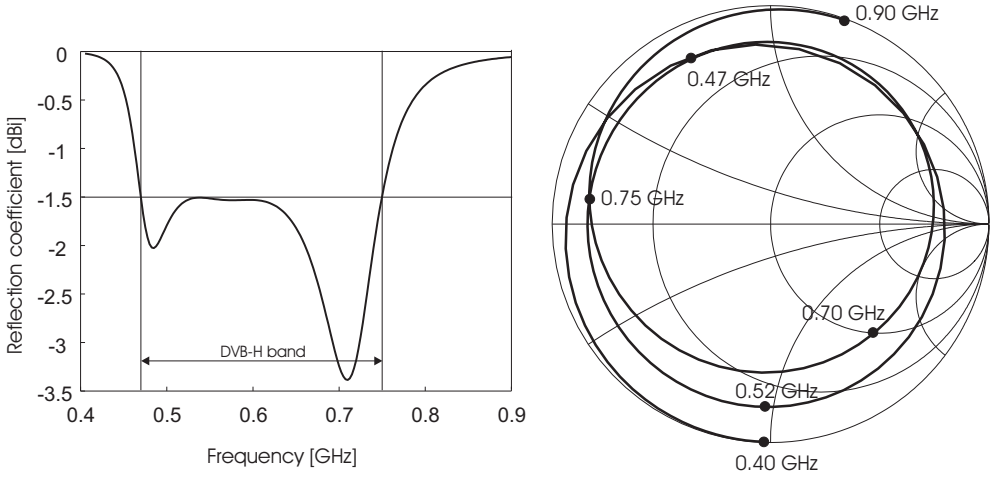

Figure 4.12: Simulated reflection coefficient a) in the Cartesian coordinate system and b) on the Smith chart.

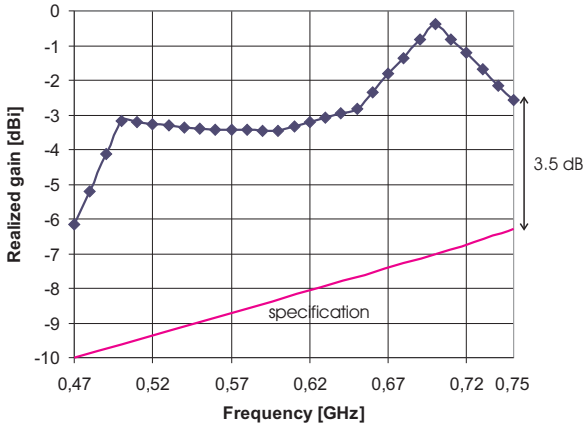

Figure 4.13: Simulated realized gain.

As shown in Figure 4.12a, the return loss is at least 1.5 dB across the DVB-H band. On the Smith chart, in Figure 4.12b, the reflection coefficient has a double loop around the center indicating fairly optimal frequency response, see Figure 3.7. According to Figure 4.13, the margin to the realized gain specification is at least 3.5 dB.

4.4 DVB-H antennas based on direct feed

Direct-feed-based DVB-H antennas have obtained interest around the world. For example the research group led by K.-L. Wong has designed and manufactured a direct-feed-based antenna prototype for a large clamshell terminal [29]. As presented in Chapter 3, direct feed antennas couple efficiently to the chassis lowest order wavemode and enable very low-profile antenna structures. This section introduces a couple of DVB-H antenna implementations based on the direct feed principle.

4.4.1 Prototype antenna

The implementation of a direct-feed-based DVB-H antenna in a tablet-size terminal is studied and demonstrated in [30]. As was presented in Chapter 3, the most optimal place of the feeding slot from the antenna operation point of view would be in the middle because the coupling to the chassis wavemode would be the strongest and consequently the achievable bandwidth largest. However, we often prefer to allocate the middle of the tablet for the display, not the feeding slot, see Figure 4.14. Thus, different locations for the feeding slot and an other slot, which decreases the resonant frequency of the lowest order wavemode, are studied. Distance d between the slots (see Figure 4.14) has a significant effect on the resonant frequency, the matching at the resonant frequency and the available bandwidth. In Figure 4.15 there are the impedance curves for the three different cases (d is 50, 70 and 90 mm) for the structure shown in Figure 4.14 presented on the Smith chart. Case $d = 70$ mm, which leads to resonance at 675 MHz, has been found to be a good compromise between the performance of the antenna and the possible display size [30]. In this

design, the width of the display unit can be 70 mm. Broader slots ($>$ 3 mm) and narrower strips ($<$ 3 mm) would yield higher performance for the antenna [30]. The location of the feed in the slot does not significantly affect the performance of the antenna and thus, the feed is placed in the middle of the slot. As the matching is not very good at the lower DVB-H frequencies (around 500 MHz), a matching circuit is needed to improve the matching (and the total efficiency) over the whole DVB-H band. The final antenna structure with the matching circuit is shown in Figure 4.16 and the prototype manufactured is shown in Figure 4.17.

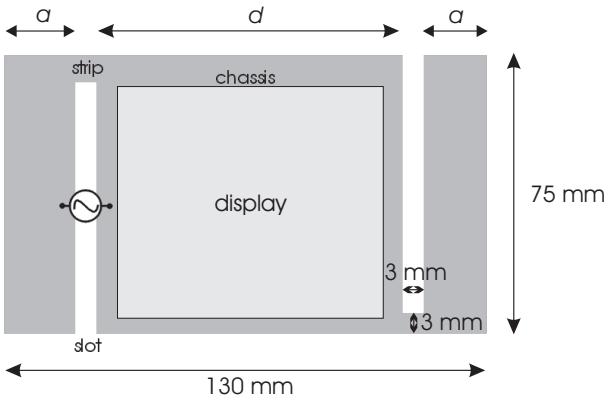

Figure 4.14: Direct-feed-based DVB-H antenna for a tablet-size terminal.

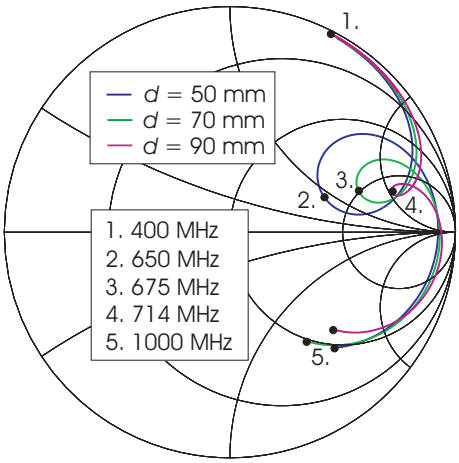

Figure 4.15: Impedance curves (400 - 1000 MHz) of the direct feed antenna structure with d = 50, 70 and 90 mm [30].

The reflection coefficient of the antenna structure is shown in Figure 4.18. As can be seen, about 1.5 dB return loss is achieved across the DVB-H band 0.47 - 0.702[4] GHz.

[4]This prototype was also manufactured in 2005 when the DVB-H band was limited to 0.702 GHz if GSM900 was used in the same terminal.

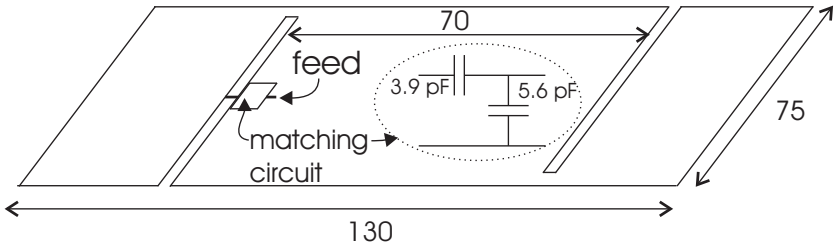

Figure 4.16: Direct-feed-based DVB-H antenna for a tablet-size terminal [30].

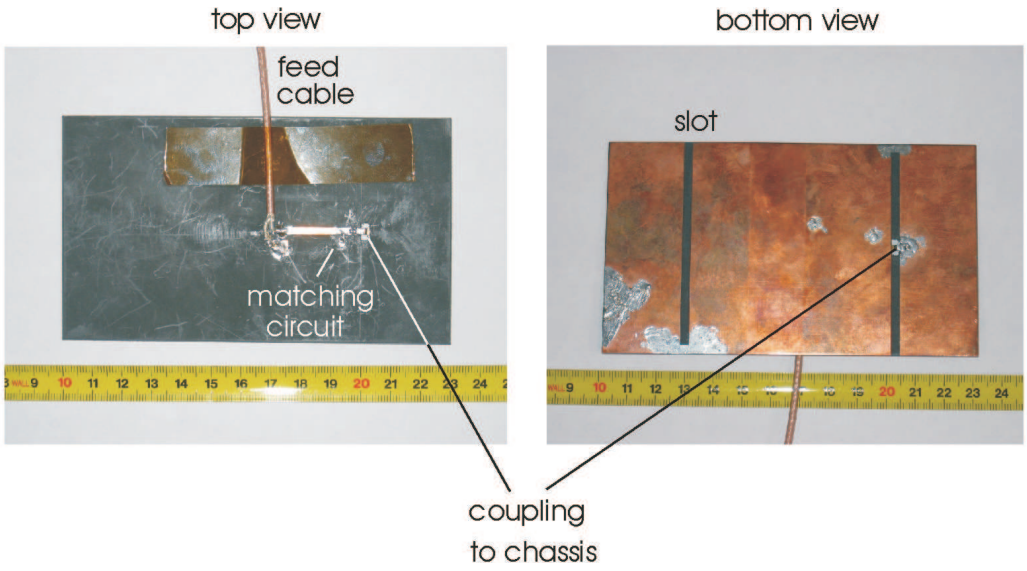

Figure 4.17: Prototype of the direct-feed-based DVB-H antenna for a tablet-size terminal [30].

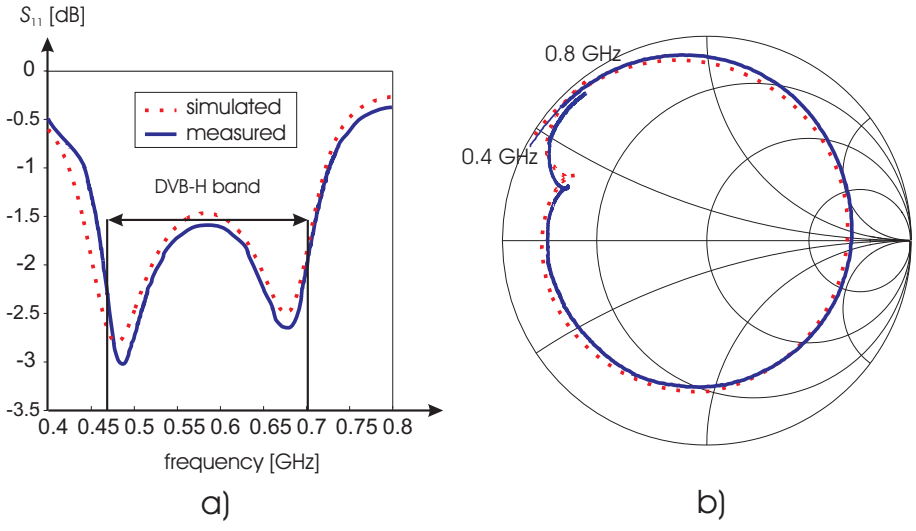

Figure 4.18: Simulated and measured reflection coefficient of the direct-feed-based DVB-H antenna a) in the Cartesian coordinate system and b) on the Smith chart [30].

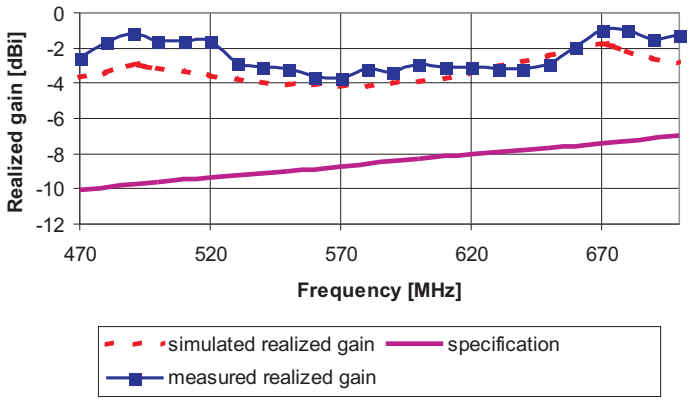

Figure 4.19: Simulated and measured realized gain of the direct-feed-based DVB-H antenna [30].

Although the matching circuit is single-resonant, the frequency response is anyway dual-resonant. However, based on the results shown in Figures 3.6 and 3.7 and also in [12], one can see from the Smith chart presentation that the dual-resonant operation is not optimal. The main problem is that instead of having the optimal loop around the Smith chart centre, there is only a small dip at 0.675 GHz indicating clearly too weak coupling to the chassis wavemode (compare with Figure 3.6). The reason for that is the location of the feed slot far away from the optimum location, the middle of the chassis. The second problem is that the resonant frequency of the chassis (about 0.675 GHz) is not equal to the centre frequency of the DVB-H system (0.586 GHz) (compare with Figure 3.7). The reason for this is that with the required mechanical structure (the display is placed between the slots) it is not possible to add more slots to the chassis in order to decrease its resonant frequency even more. Nevertheless, the performance of the antenna is very good, 4 dB above the specification, see Figure 4.19. The radiation pattern is similar to that of a dipole antenna and the maximum directivity is about 2 dBi. It is difficult to compare occupied volumes of capacitive coupling element and direct feed antennas in Figures 4.5 and 4.16. However, both antenna structures (see also Figure 4.10) are very thin in size.

4.4.2 Simulated design for open clamshell terminal

Since the antenna structure presented in [29] is for rather large clamshell terminals, this subsection presents a simulated design for typical-size clamshell handsets available today [1], see Figure 4.20. The length of the antenna structure in the open position is large in wavelengths ($0.34\lambda_0$ at the center frequency 0.610 GHz) and the feeding slot is in the middle and thus relatively good performance can be expected. Simulated reflection coefficient and realized gain are presented in Figures 4.21 and 4.22, respectively. Since the simulations and measurement results of the manufactured prototype presented in Figures 4.16 and 4.17 agreed very well, similar agreement would be expectable also with a possible prototype based on the design presented here.

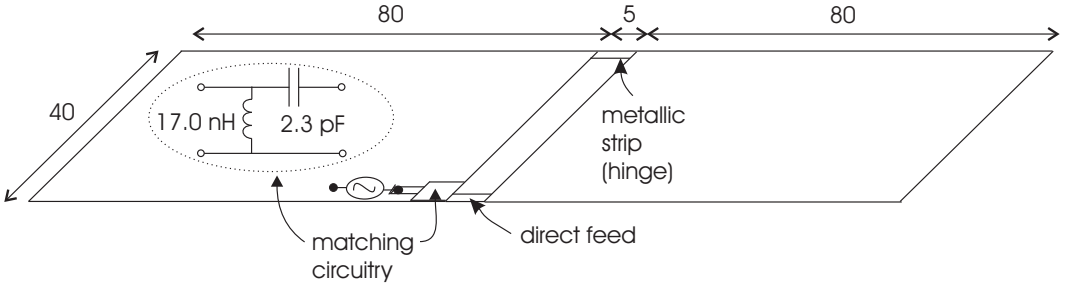

Figure 4.20: Simulated DVB-H antenna design for a today's typical-size open clamshell terminal.

As can be seen in Figure 4.21a, return loss better than 1.8 dB is achieved. The effect of the chassis lowest order wavemode can be noticed on the Smith chart in Figure 4.21b at about 0.75 GHz, where such 'rise' can be recognized and due to that the frequency response is dual-resonant although the matching circuit is inherently single-resonant. Anyway, the frequency response of the reflection coefficient on the Smith chart is neither here optimal from the bandwidth point of view (compare with Figures 3.6 and 3.7). However, according to Figure 4.22, the margin to the realized gain specification is at least 6 dB.

In the clamshell-type antenna presented in [29] the margin to the realized gain specification was 9 dB with the structure whose length in the use position (clamshell open) is 200 mm. According to the simulated design presented in this work the mar-

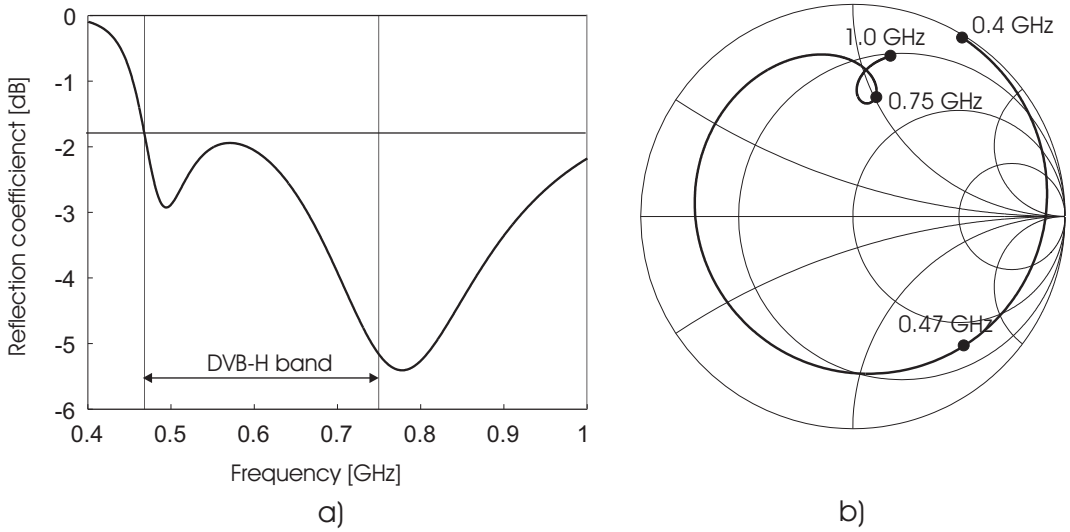

Figure 4.21: Simulated reflection coefficiecnt of DVB-H antenna design for a clamshell terminal a) in the Cartesian coordinate system and b) on the Smith chart.

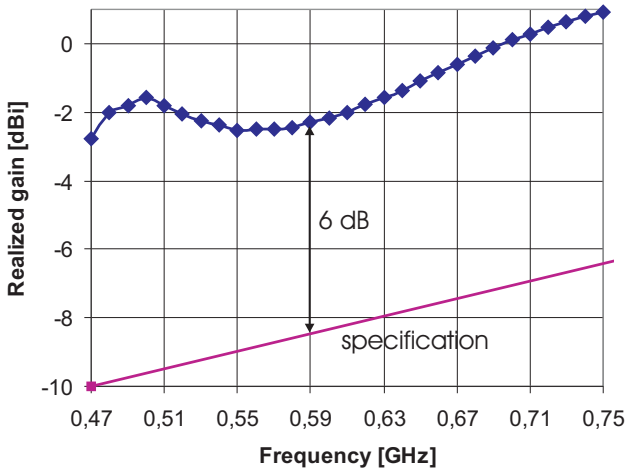

Figure 4.22: Simulated realized gain of DVB-H antenna design for a clamshell terminal.

gin to the specification is 6 dB with the use position (clamshell open) length of 165 mm. Thus, decreasing the clamshell size is not very crucial for the performance of the antenna. Compared to the capacitive coupling element implementation, see Figure 4.10, both direct feed and coupling element antenna solutions are very compact and thin in size. Direct feed based DVB-H antennas are very potential candidates for clamshell handsets since they can also provide excellent performance.

4.5 Effect of the user on DVB-H antennas

DVB-H needs to work in all possible positions and places. The main objective of the study in this section [46] is to verify that the DVB-H antenna prototypes are usable when the terminal is either held by the user or it is located in free space. The effect of the user on matching, radiation and total efficiencies, and realized gain are presented.

4.5.1 Hand models, simulation tools and settings

The effect of the user was studied by comparing the results from free space simulations with results when the terminal was held either with left or right hand alone or with both hands, see Figure 4.23. The study was performed with the capacitive coupling element and direct feed antennas shown in Figures 4.5 and 4.16, respectively.

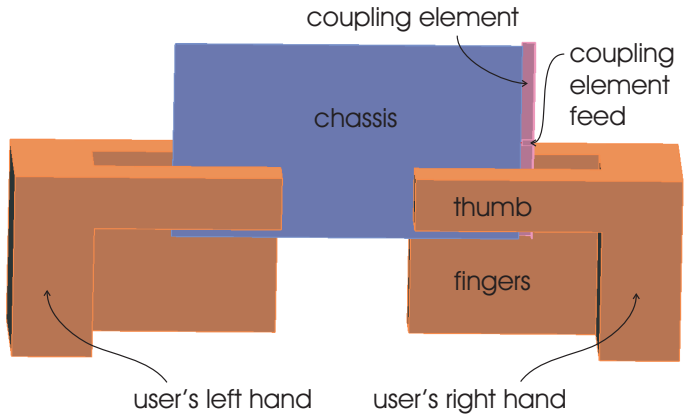

Figure 4.23: Two-hand grip of a terminal with a coupling element based DVB-H antenna.

The hands were modeled on dielectric material having electrical properties of the muscle tissue ($\varepsilon_{reff} = 56$ and $\sigma_{eff} = 1$ S/m [45]) averaged over the simulation frequency band (0.45-0.8 GHz). The effective conductivity σ_{eff} is approximately constant over the used frequency band because the muscle tissue has a high water content and the changes in the effective permittivity ε_{reff} are also small. Due to the material parameters of the bones [45], they do not absorb RF power strongly

[26]. As the bones are not modeled here, this analysis yields the worst case scenario. The most critical dimension in the hand models is the distance between the thumb and the rest of the fingers, i.e. the thickness of a terminal. In the simulations the thicknesses of 10 mm and 20 mm were used. 10 mm was considered to be the smallest possible thickness of a terminal. Those results will be presented here to give the worst case scenario results.

The metal parts were modeled as perfect electric conductors (PEC) and thus all the losses are caused by the hands. In a more realistic case the conductivity and dielectric losses of the antenna structure and the matching circuit component losses would decrease the radiation efficiency and make the interpretation of the results more difficult and less useful.

The dimensions of the coupling element antenna and the hand models are shown in Figures 4.24 and 4.25 and the corresponding dimensions for the direct feed antenna are shown in Figures 4.26 and 4.27. The matching circuits are not shown in the figures.

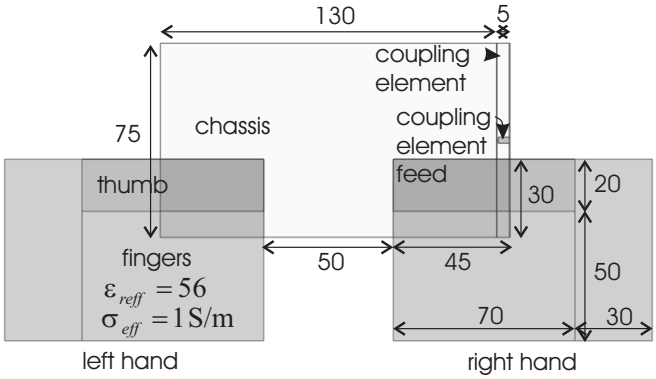

Figure 4.24: Front view of the coupling element based DVB-H antenna in user's hands. Dimensions are in mm.

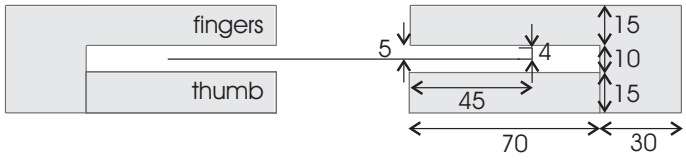

Figure 4.25: Top view of the coupling element based DVB-H antenna in user's hands. Dimensions are in mm.

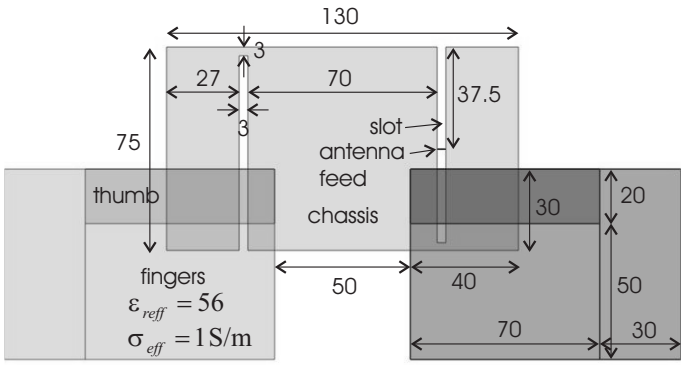

Figure 4.26: Front view of the direct based DVB-H antenna in user's hands. Dimensions are in mm.

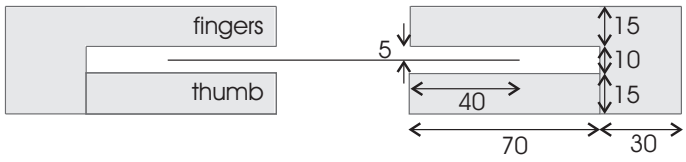

Figure 4.27: Top view of the direct feed based DVB-H antenna in user's hands. Dimensions are in mm.

The study was performed with SEMCAD X (version 11.0), which is an FDTD-based electromagnetic simulator [44]. The maximum FDTD-mesh cell size in the antenna and hand models was $\Delta x = \Delta y = \Delta z = 1.0$ mm. The smallest wavelength in the hand tissue at the simulation band is 50.1 mm. Since the maximum diagonal of the cell is $\Delta x \cdot \sqrt{3} = 1.73$ mm, there are at least 28 cells per wavelength. That was found to be a good compromise between the simulation accuracy and a reasonable simulation time. In free space the maximum cell size was 10 mm.

4.5.2 Effect of the user on matching

To be able to see the change of the chassis lowest order resonant frequency due to the user, the reflection coefficients of the antenna structures were simulated without the matching circuitries. The reflection coefficients in free space, the terminal held with left or right hand alone or with both hands are shown in Figures 4.28.

The resonant frequency of a coupling element and 130 mm-long solid chassis combi-

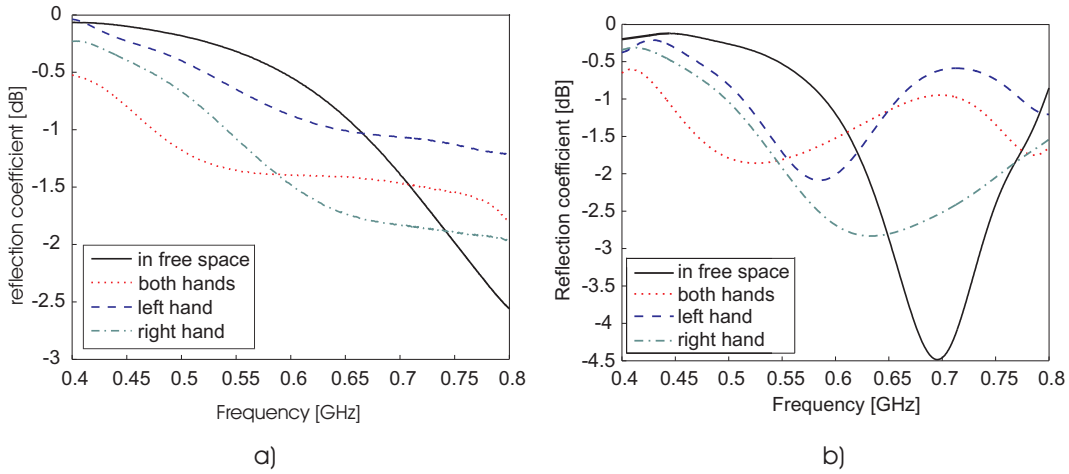

Figure 4.28: Effect of the user on the reflection coefficients of a) the coupling element and b) direct feed based DVB-H antenna structures without the matching circuit.

nation in free space is about 0.9 GHz, see (3.4). As can be seen from Figure 4.28a, the hands decrease the resonant frequency of the antenna structure. The hand consisting of dielectric material increase the capacitance of the resonator formed by the chassis and coupling element combination and thus the resonant frequency decreases. The resonant frequency is the lowest (about 0.6 GHz) when the antenna is held with both hands. The resonant frequency also decreases with the direct feed antenna, see Figure 4.28b.

The matching circuits were not included in the simulations in SEMCAD X because no validated results of the lumped element FDTD simulations with SEMCAD X were found. Instead, the reflection coefficients of the unmatched antennas simulated in free space were exported from SEMCAD X to AWR APLAC circuit simulator [43] which was then used for the matching circuit design. The matching circuits used are shown in Figure 4.29. The component values of the matching circuits differ from those used in the manufactured prototypes (see Figures 4.6a and 4.16) because in this study simplified simulation models of the antennas and ideal matching circuit components were used. Finally, the reflection coefficients of the antennas with user's hands were simulated and imported to AWR APLAC and the reflection coefficients with the matching circuits (designed in free space) were simulated. The results are shown in Figure 4.30

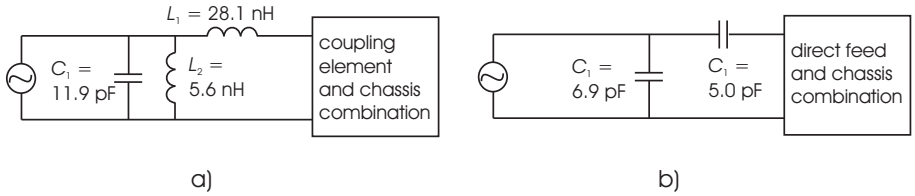

Figure 4.29: Matching circuits used for the a) coupling element and b) direct feed based DVB-H antennas.

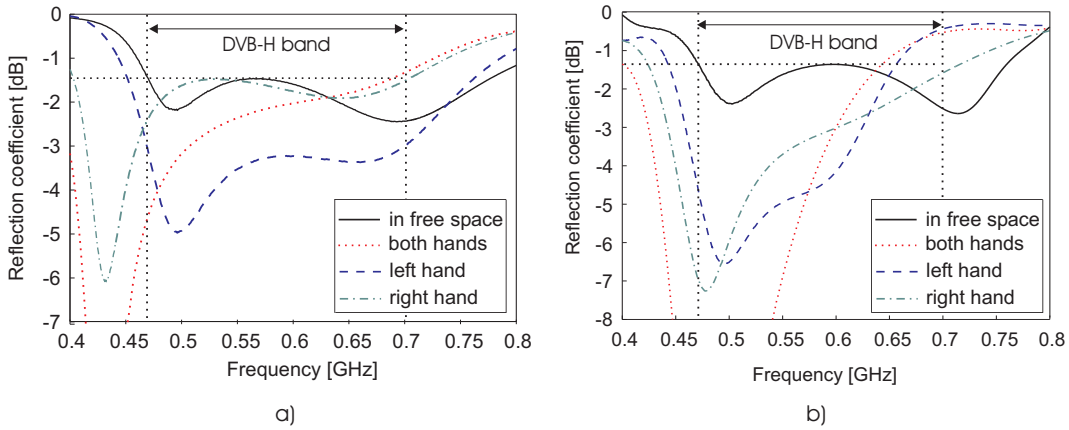

Figure 4.30: Effect of the user on the reflection coefficients of the a) coupling element and b) direct feed based DVB-H antenna structures with the matching circuit.

As can be seen in Figure 4.30a, the detuning of the matching of capacitive coupling element antenna caused by the hands seems not very problematic. In fact, the matching with the left hand grip is clearly better than in the free space case. In the other cases the matching is worse compared to the free space case only around 0.5 GHz with right hand and around 0.7 GHz with right and both hands. According to Figure 4.30b, the detuning of the matching seems to be a clearly larger problem in the direct feed antenna than in the coupling element antenna. In the worst case, at the upper edge of the band, the return loss is deteriorated dramatically. By redesigning the matching circuit, e.g. using triple-resonant matching, the effect of the detuning may be decreased.

4.5.3 Efficiency and gain simulations

The radiation and total efficiencies with different hand grips were simulated and the results for the coupling element antenna are shown in Figure 4.31.

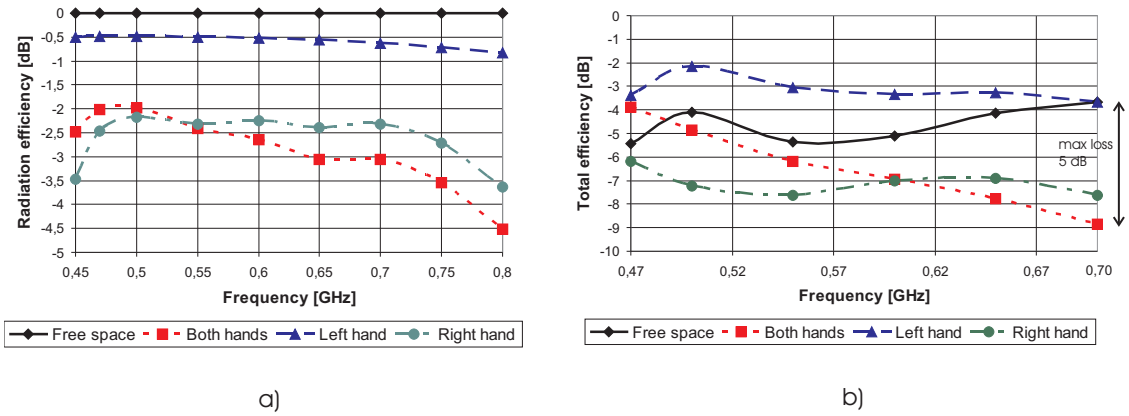

Figure 4.31: a) Simulated radiation and b) total efficiencies for the coupling element DVB-H antenna. The markers are the simulated frequencies.

As can be seen in Figure 4.31a, the hand or hands decrease the radiation efficiency 0.5 - 3 dB at the DVB-H band. The decrease in the radiation efficiency was the smallest when the terminal was held with the left hand. This could be expected because the coupling element is at the other end of the chassis. As can be seen in Figure 4.31b, the total efficiency is higher with the left hand grip than in free space. That is possible, because improvement in the matching on the moderate matching level (1...2 dB return loss, see Figure 4.30) causes relatively large improvement in the matching efficiency, see (2.7). The total efficiency increases because the improvement in the matching efficiency more than compensates the decrease of the radiation efficiency. The decrease in the total efficiency was largest with right hand when averaged over the DVB-H band. The worst single case occurred at the upper edge of the band when the terminal was held with both hands. In that case the total efficiency decreases by 5 dB at the maximum compared to the free space case.

The simulated realized gains for the coupling element DVB-H antenna are presented in Figure 4.32. As can be seen, the margin to the specification in the simulated free-space case is about 5 dB, whereas in the manufactured prototype introduced in Figure 4.5 the margin was 4 dB. This difference is due to the fact that the antenna structure and the matching circuit are now lossless in the simulations. In all the simulated cases the realized gain is above the specification at least by 1.5 dB. The simulated directivity in free space is 2.2 dBi at 0.70 GHz and the radiation pattern is similar to that of a dipole antenna. The simulated directivity with both

hands is 3.2 dBi at 0.70 GHz. The hands cause distortion on the radiation pattern and thus the directivity increases compared to the antenna in free space. This causes an extra increment (1 dB) in the realized gain, which gives the impression that the performance of the antenna seems to be better than it actually is. This indicates that the realized gain seems not to be a very good measure for the antenna performance in this case. A more realistic measure for the antenna performance might be mean effective gain (MEG), which takes into account the radiation pattern and polarization of the antenna and the incident waves [47]. However, according to the simulated results the capacitive coupling element antenna seems to tolerate fairly well the presence of the user.

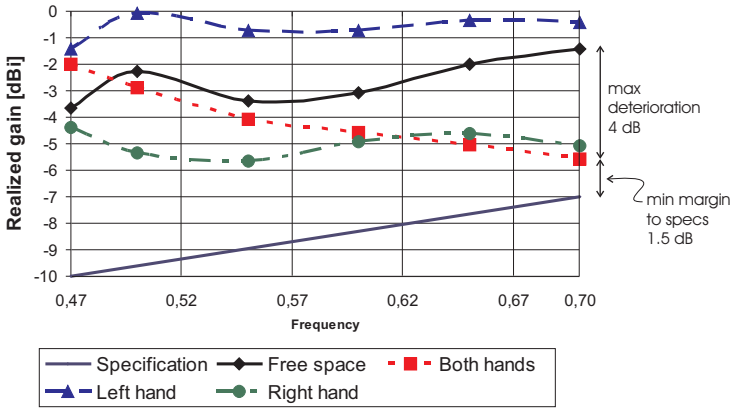

Figure 4.32: Simulated realized gain for the coupling element DVB-H antenna. The markers are the simulated frequencies.

The simulated efficiencies and realized gains for the direct feed antenna are shown in Figure 4.33 and 4.34, respectively.

As can be seen in Figure 4.33a, the radiation efficiency of the direct feed antenna decreases 0.7 - 3.5 dB when comparing to the free space case. That is only 0.5 dB worse than with the capacitive coupling element antenna. A clear correlation can be seen between the radiation efficiencies and the reflection coefficients of the direct feed and chassis combination, see Figures 4.33a and 4.28b: The radiation efficiency maxima are reached approximately at the resonant frequencies of the direct feed and chassis combination. To be able to draw further conclusions from this, more simulations should be done. Due to the considerably improved matching below 0.6

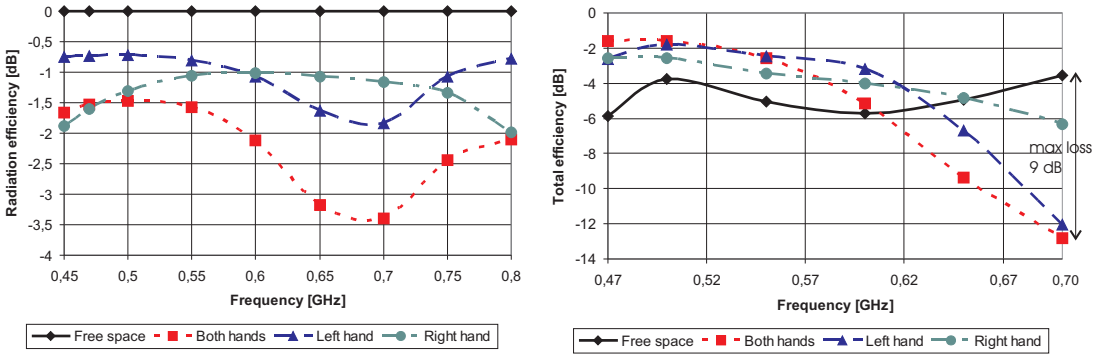

Figure 4.33: a) Simulated radiation and b) total efficiencies for the direct feed DVB-H antenna. The markers are the simulated frequencies.

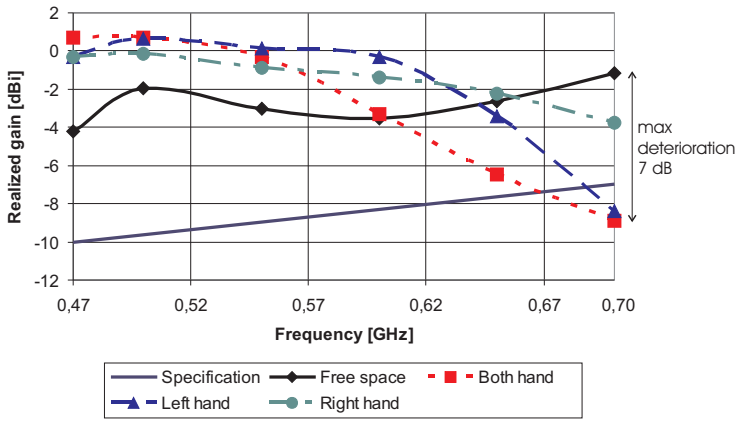

Figure 4.34: Simulated realized gain for the direct feed DVB-H antenna. The markers are the simulated frequencies.

GHz (see Figure 4.30b), the total efficiency of the direct feed antenna improves in all cases compared to free space case below 0.6 GHz. On the other hand at the upper edge of the band, the total efficiency of the direct feed antenna drops dramatically, by 9 dB at the maximum, which is 4 dB worse than in the case of the capacitive coupling element antenna. The realized gain drops 2 dB below the realized gain specification, see Figure 4.34. Thus, the direct feed antenna seems to be more challenging from the user effect point of view than the capacitive coupling element antenna. However, since the decrease of the radiation efficiency seems not to be very bad with the direct feed antenna, the redesign of the matching circuit may decrease the effect of the detuning of the matching and thus the total efficiency, and consequently the realized gain would stay more even across the band.

4.6 Interoperability of DVB-H and transmitting systems in the same terminal

The coupling between different antennas in a handheld terminal is problematic. Firstly, it may cause unwanted interference between different transmitting and receiving systems and in the worst case the operation of the receiving system is even impossible. Secondly, the radiation efficiencies of the antennas decrease since the other antennas capture a part of the power that would normally be radiated or received. Thirdly, the design of antennas cannot be done independently for each antenna. Thus, the largest possible isolation between antennas is desirable since it decreases the need for expensive and lossy filters in the input of the systems. In addition, in the case of MIMO systems, the mutual coupling usually also reduces the MIMO capacity performance.

Interoperability of DVB-H with the transmitting systems, such as GSM900, GSM1800, UMTS and WLAN, is desired. For example, data downloading may be running through DVB-H in parallel to a phone call, and thus the simultaneous operation of DVB-H and GSM900/1800 is desirable. In this section the interoperability of DVB-H and transmitting antennas in a handheld device is analyzed and possible solutions to overcome the problem are discussed.

4.6.1 Electromagnetic isolation

Since the total isolation between antennas is affected also by the matching, it is difficult to compare the isolation between two antenna elements for different cases. To be able to exclude the matching from the total isolation, the concept of *electromagnetic isolation* is introduced in [48]. It means the 'worst-case' isolation, which is independent of matching. The electromagnetic isolation is calculated as follows. The S parameters of a two-port antenna structure are simulated or measured. Using the S parameters, both antennas are simultaneously conjugately matched at the same frequency. Since the reflections in the antenna elements are this way canceled, the maximum power is transferred between the antenna elements, i.e. the maximum

power is lost in the other antenna feed. The formulas for the above-described process are given e.g. in [5] and [11]. For passive antenna structures the power transfer in decibels is smaller than 0 dB and the electromagnetic isolation is defined as the power transfer with the opposite sign.

Figure 4.35 presents the antenna structure studied in this interoperability study. The capacitive coupling element on the right-hand side is for DVB-H is similar to the one used in Chapter 4. The coupling element on the left-hand side is used for the transmitting systems, in this case for GSM900, GSM1800, UMTS or WLAN/Bluetooth. The implemenation of capacitive coupling element antennas for the GSM900 and GSM1800 is studied in detail in [23]. The two-antenna structure shown in Figure 4.35 is considered to present a possible antenna placing in mobile terminals.

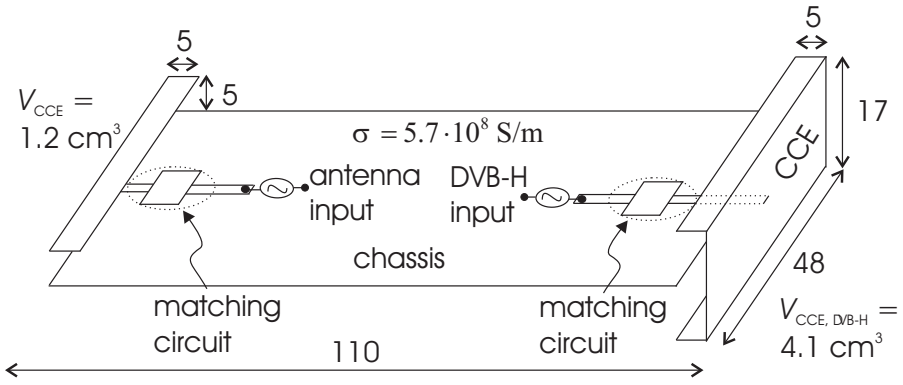

Figure 4.35: Antenna structure used in the interoperability study.

The electromagnetic isolation is calculated for the two-antenna structure. The S parameters (without any matching circuits) are simulated with IE3D [18] over the frequency range 0.4-5 GHz. The simultaneous conjugate matching and the maximum power transfer are calculated at each simulated frequency using the formulas given in [11]. The electromagnetic isolation is presented in Figure 4.36 and for some relevant frequencies reported in Table 4.4.

As can be seen, below 1 GHz the isolation is less than 2 dB, which means that the other antenna captures more power than what is radiated. Thus, the antenna elements are electromagnetically very strongly coupled. Actually, this low isolation can be explained. As discussed earlier in Chapter 3, the chassis is the main radiator below 1 GHz and thus to be able to reach sufficient bandwidth, both antenna elements

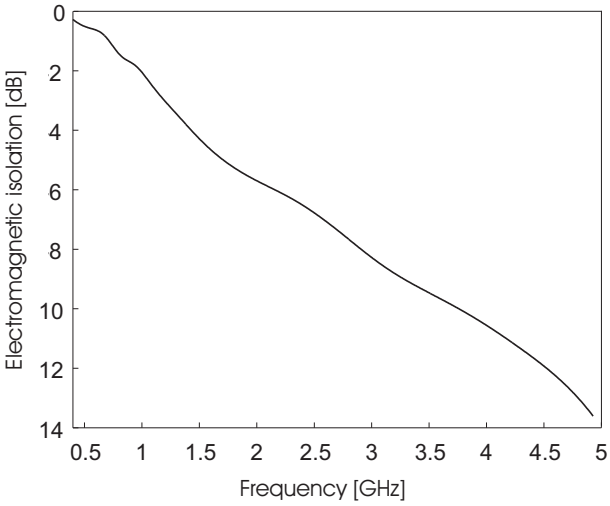

Figure 4.36: Electromagnetic isolation for the two-port antenna structure.

Table 4.4: Electromagnetic isolation values for the two-port antenna structure.

frequency [GHz]	electromagnetic isolation [dB]
0.47	0.45
0.75	1.2
0.88	1.7
0.96	1.9
1.71	5.0
1.88	5.4
1.92	5.5
2.17	6.0
2.4	6.5
2.5	6.8

are strongly coupled to the chassis. This way the antenna elements are strongly coupled to each other through the chassis. This can also be understood in terms of resonator-based analysis discussed in Section 3.3. In the equivalent circuit shown in Figure 3.5, the single antenna element (parallel RLC resonator) was coupled to the chassis (series RLC resonator). An equivalent circuit for the two-port system, in which the antenna elements are coupled mainly through the chassis, is shown in Figure 4.37. The equivalent circuit can be used in the vicinity of the chassis lowest

order wavemode resonant frequency f_{rc} which is for a 105 mm-long chassis about 1.1 GHz, see (3.4).

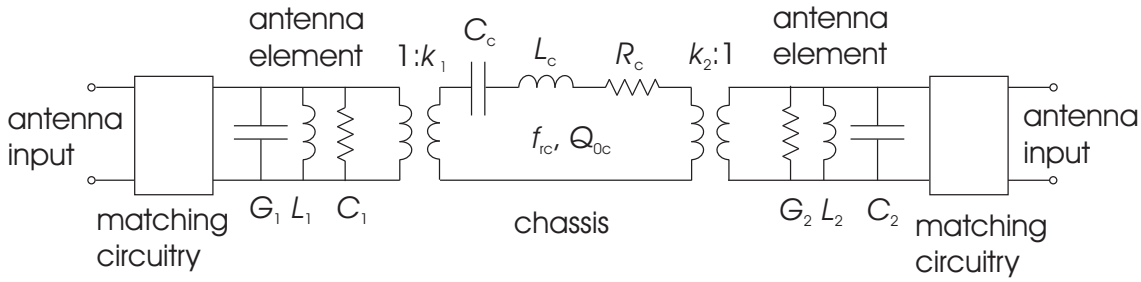

Figure 4.37: Equivalent circuit of the two-port antenna system.

Different locations and shapes of the antenna elements were tested with simulations (not shown here) but the level of the isolation remained approximately the same, i.e. worse than 2 dB. It can be concluded that since the electromagnetic isolation does not very much depend on the antenna elements, one cannot improve the electromagnetic isolation by mere antenna (element) design. Logical next step of the attempt to improve the electromagnetic isolation would be to study how the currents induced by single antenna element could be isolated on the chassis.

Since the chassis is the main radiator below 1 GHz, any antenna elements used for DVB-H and GSM900 need to be strongly coupled to the chassis. Thus, the capacitive coupling elements used in this study do not limit the study and the results would be in the same order also with other kind of antenna elements such as PIFAs.

4.6.2 Antenna design for DVB-H and GSM900

In practice DVB-H and GSM900 antennas are not matched at the same frequencies and thus the total isolation is usually better than the corresponding electromagnetic isolation. To maximize the isolation, the reflection coefficient of the DVB-H antenna should be as large as possible at the GSM900 frequency band and vice versa.

This subsection presents an example antenna design for DVB-H and GSM900 in the same terminal. The purpose of this design is to demonstrate the isolation value that can be expected in practice. The antenna structure is shown in Figure 4.35. The

DVB-H antenna matching circuit in this design is the same as used in Chapter 4. For GSM900 a dual-resonant matching circuit with ideal lumped element components is shown in Figure 4.38. The simulated reflection coefficients are shown in Figure 4.39 and the isolation between antennas is shown in Figure 4.40. The realized gain for DVB-H and the radiation and total efficiencies for GSM900 are presented in Figures 4.41.

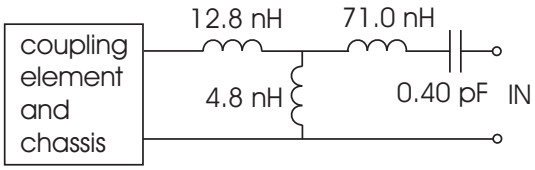

Figure 4.38: Antenna structure used in the interoperability study.

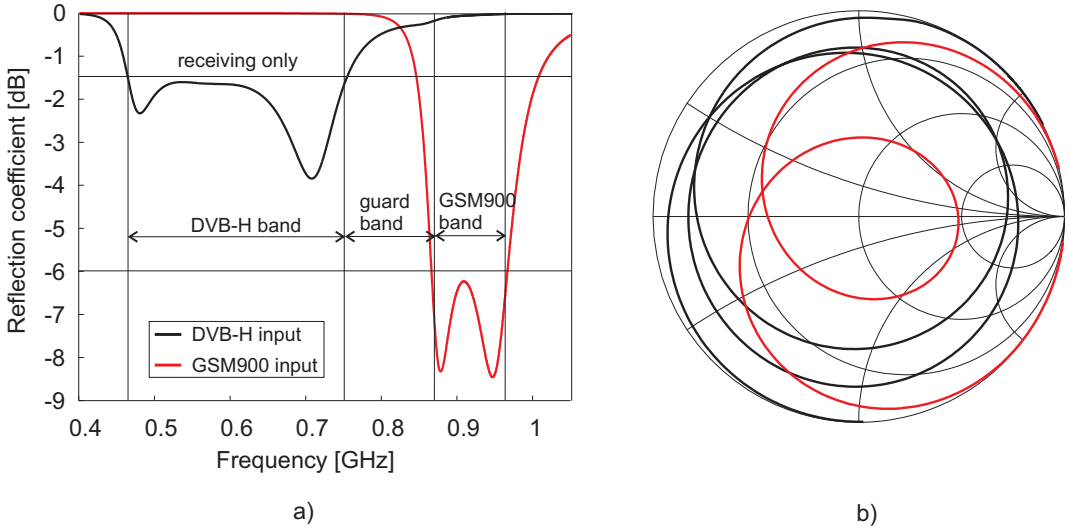

Figure 4.39: Reflection coefficients for both antennas a) in the Cartesian coordinate system and b) on the Smith chart.

As can be seen the minimum isolations are about 27.7 and 18.6 dB at the DVB-H and GSM900 band, respectively. Thus, the matching circuits can improve the total isolation by about 16 dB compared to the electromagnetic isolation at the GSM900 band. In this example if the GSM900 transmit at its maximum power level, i.e. 33 dBm, about 15 dBm (31.6 mW) would be coupled to the DVB-H receiver and the operation of DVB-H would be impossible [35], [36], [49] . Thus, to make the simultaneous operation possible, more isolation is needed. Trivial solution from the antenna point of view is to put a GSM reject filter in the input of the DVB-H

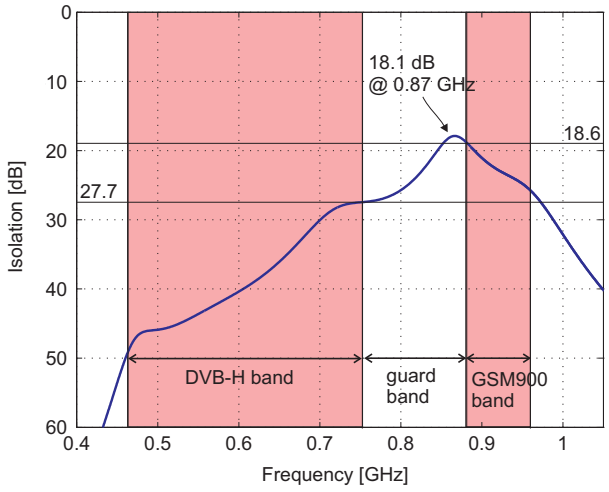

Figure 4.40: Total isolation between antennas.

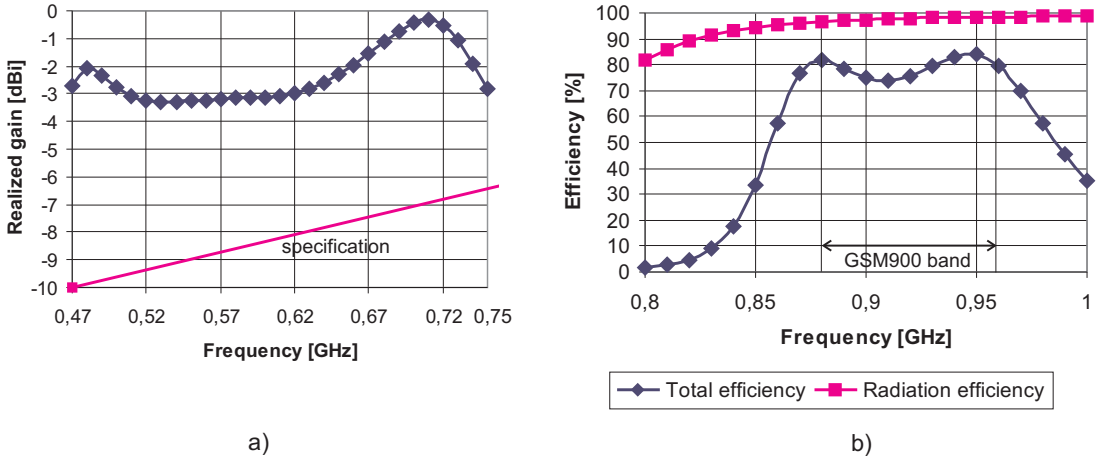

a) b)

Figure 4.41: a) Realized gain of the DVB-H antenna and b) radiation and total efficiencies of the GSM900 antenna.

receiver. An alternative solutions has been demonstrated in [50] where a combined matching and filtering circuitry comprises a strong GSM trap that attenuates the GSM frequencies by more than 40 dB. The next step of the antenna design presented in this section would be to design and implement a matching circuit that improves the isolation between DVB-H and GSM900 antennas.

4.6.3 Isolations between DVB-H and the other transmitting systems

To demonstrate practical isolation values the operation of DVB-H with other transmitting systems (GSM1800, UMTS and WLAN/Bluetooth) was simulated the same way as it was done with GSM900 in the previous subsection. The total isolations are reported in Table 4.5. Since the electromagnetic isolation between antenna elements at GSM1800, UMTS and WLAN/Bluetooth bands is 5.0 - 6.8 dB, it can be noticed that the simple matching circuits improve the total isolation at the transmitting band at least by 47 dB. Finally, it can be concluded the other transmitting systems are not very critical from the interoperability point of view since the isolation is rather high.

Table 4.5: Total isolation values between DVB-H and other transmitting systems.

DVB-H versus	Min. isolation at DVB-H band (0.47-0.75 GHz) [dB]	Min. isolation at the transmitting band [dB]
GSM1800	36.8	52.7
UMTS	36.7	56.8
WLAN/Bluetooth	33.3	64.6

Chapter 5

Summary of the work

The work starts in Chapter 2 with small-antenna fundamentals, basic single-resonant matching circuit design and impedance bandwidth enhancement methods. Since the size of the antenna is limited inside a mobile terminal and the total efficiency should be as high as possible, the basic challenge an antenna designer is handling with is the inherently narrow impedance bandwidth.

In the beginning of Chapter 3 it is presented that the electrically largest metal piece, the chassis, of a mobile terminal contributes very remarkably to the radiation below 1 GHz. Since the antenna element is only a minor radiator, the size of the antenna element can be decreased remarkably by using compact coupling structures which couple to the dominating wavemodes of the chassis. The resonance of the antenna is produced outside the antenna structure with an external (single-resonant or multi-resonant) matching circuitry. Chapter 3 introduces in detail two different compact coupling structures, capacitive coupling element and direct feed. Capacitive coupling elements couple to chassis wavemodes via electric fields and direct feed antennas galvanically across an impedance continuity formed e.g. by a slot. Based on the results, guidelines for the optimum shaping and location of both compact coupling structures are given. Both compact coupling structure antennas are shown to provide the same or even larger impedance bandwidth as in the case of the presented reference PIFA antenna but they occupy considerably smaller volume than the reference. Especially direct feed structures are shown to provide very low-

profile antenna solutions. Although the volume of the direct feed structure is almost zero, the effective volume of the antenna is not zero because no conductive elements can be placed over the feeding slot. It is also shown in Chapter 3 that impedance bandwidth maxima are achieved at the chassis wavemode resonant frequencies. By modifying the chassis shape, e.g. by making slots, it was shown to be possible to optimize the chassis wavemode resonant frequencies.

Chapter 4 presents the main results of the work. In the beginning, the design aspects of the DVB-H antennas are discussed. It is presented that to be able to implement a feasible-size DVB-H antenna inside a mobile handset, the total efficiency of the antenna needs to be sacrificed. However, it is also estimated based on the calculations that an antenna which has considerably reduced total efficiency, is capable of providing a sufficient signal-to-noise ratio for the whole DVB-H receiver system. The specification of the DVB-H antenna performance, which takes into account both feasible size and sufficient total efficiency, is introduced in terms of realized gain. In this work the total efficiency is sacrificed by accepting some mismatching. Since DVB-H is receiving only, some mismatching may be tolerable unlike in transceiver antennas. In real handsets, other parts like plastic covers, display, battery and possible GSM reject filter would introduce certain implementation losses and thus matching would be improved. To compensate the implementation losses a suitable margin to the realized gain specification is needed in simplified prototypes and designs presented in this work. 3 dB was considered to be the sufficient margin in this work.

A capacitive coupling element based DVB-H prototype antenna (volume 1.5 cm^3) was presented for a tablet-size terminal in Chapter 4, see Figure 4.5. The capacitive coupling element implementation has already been commercially interesting since DVB-H antennas are designed and manufactured by Pulse Finland Oy (volume 1.5 cm^3) and Fractus (volume 2.6 cm^3), see Figure 4.7. The smallest possible size of coupling element antenna structures, which have the chassis dimensions of the today's handsets and also a sufficient margin to the realized gain specification, were studied in Chapter 4. Based on the results, generally rather big and high coupling elements compared to the existing commercial antennas were needed to reach the sufficient margin with typical-size terminals, see Figure 4.10 and Table 4.3. A sim-

plified coupling element based DVB-H antenna design for a typical-size terminal with sufficient performance margin was demonstrated, see Figure 4.11.

A very thin direct-feed-based DVB-H prototype antenna with a 4-dB margin to the specification was presented for a tablet-size terminal in Chapter 4, see Figure 4.16. As was discussed in Chapter 3, direct feed antennas fit inherently well for clamshell terminals. A simplified DVB-H antenna design for a typical-size clamshell terminal with 6-dB margin to the realized gain specification is also demonstrated in Chapter 4, see Figure 4.20.

The effect of the user on the matching, the radiation and total efficiencies, and the realized gain was studied for capacitive coupling element and direct feed prototype antennas in Chapter 4. The change of the matching due to the hands seems not to be a very big problem with the capacitive coupling element antenna. The direct feed antenna seems to be more difficult since the matching around 0.70 GHz is dramatically deteriorated with certain hand grips. The radiation efficiency of the coupling element antenna decreases by 3 dB at the maximum and the total efficiency by 5 dB when comparing to the free space case. Due to the hands the directivity of the antenna increases compared to free space case. This causes an extra increment in the realized gain and thus the performance of the antenna seems better than it actually is. This indicates that the realized gain may not to be a very good measure for the antenna performance in the effect of the user study.

The capacitive coupling element antenna seems to tolerate fairly well the presence of the user. The radiation efficiency of the direct feed antenna decreases at the maximum by 3.5 dB compared to the free space case. Due to the considerably deteriorated matching around 0.70 GHz, the total efficiency of the direct feed antenna drops by 9 dB at the maximum at the DVB-H band, which is 4 dB worse compared to the capacitive coupling element antenna. Thus, the direct feed antenna seems to be more challenging from the user effect point of view than the capacitive coupling element antenna.

In multisystem terminals it is likely that strong signal is leaking from the GSM transmitter to the sensitive DVB-H receiver and the simultaneous operation of DVB-

H is not possible. Tens of decibels of isolation is required between the systems if the simultaneous operation is wanted. In Chapter 4 it was demonstrated that isolation of at least 18 dB was achieved between coupling-element-based DVB-H and GSM900 antennas without additional filters which means that in practice other solutions are needed than those based on antenna element shape optimization. The isolation between DVB-H and other transmitting systems that operate above 1 GHz was shown to be rather large and the interoperability seems much less problematic.

Chapter 6

Conclusions

The aim of this Licentiate thesis has been to provide a comprehensive study on the implementation of DVB-H antennas inside a mobile terminal. The results were collected from the work carried out by the author since June 2005.

Since the volume that can be reserved for antennas is very restricted, the limits for the size of capacitive coupling element based antenna structures inside handsets of different size were studied. The results indicate that the smallest required volume of the coupling element which ensures sufficient performance in today's typical-size monoblock mobile handsets would be about 3 - 4 cm^3. On the other hand, for tablet-size and open clamshell-size terminals the antenna element can be remarkably smaller and thinner. In addition, direct-feed-based structures are shown to provide very low profile antenna solutions for tablet and clamshell-type terminals. As the result of the research, four different DVB-H antenna prototypes and simulated designs were presented and evaluated. All of them are considered to be a suitable trade-off between the size of the antenna and a sufficient margin to the realized gain specification. The effect of the user on the performance of the DVB-H antenna was studied for two of the four cases. Maximum of 5 - 9 dB decrease in the total efficiency was shown and thus the effect of the user seems to be a significant challenge for the operation of DVB-H. For the case of simultaneous operation of DVB-H and GSM900 on a typical-size terminal, a relatively low isolation, about 18 dB, between the DVB-H and GSM900 antennas was demonstrated and thus the interoperability

of DVB-H and GSM900 seems impossible without additional filtering.

This work presents lots of useful information on the implementation of DVB-H antennas in multisystem handheld devices. The results provide a basis for further development of DVB-H antennas. Natural continuation of the work would be to study how to control or adjust the electrical properties of the chassis in such a way that it adapts for different systems and possibly improves the isolation between different antennas, especially between DVB-H and GSM900. The design of a combined matching and filtering circuit for a DVB-H antenna would be natural extention in developing the interoperability of DVB-H and GSM900. Logical next step of the presented effect of the user study would be measurements with prototype antennas and hand models or even real users. Simulations with commercial hand models and other simulators could be performed to be able to compare the validity of the results.

Bibliography

[1] http://europe.nokia.com/products (cited 27.3.2008)

[2] J. Holopainen, *Antenna for Handheld DVB Terminal*, Master's thesis, Helsinki University of Technology, Radio Laboratory, Espoo, Finland, May 2005.

[3] K. Fujimoto, A. Henderson, K. Hirasawa and J.R. James, *Small antennas*, New York, 1987, Research Studies Press, 300 p.

[4] A.V. Räisänen, A. Lehto, *Radio Engineering for Wireless Communication and Sensor Applications*, Artech House (Boston, Massachusetts), May 2003, 366 p.

[5] A.V. Räisänen, A. Lehto, *RF- ja mikroaaltotekniikka*, Helsinki, 2006, 271p.

[6] L.J. Chu, "Physical limitations on omni-directional antennas", *Journal of Appl. Physics*, vol. 19, 1948, pp. 1163-1175.

[7] R.C. Hansen, "Fundamental Limitations in Antennas," *Proceedings of the IEEE*, Vol. 69, No. 2, February 1981, pp. 170-182.

[8] J.S. McLean "A Re-Examination of the Fundamental Limits on the Radiation Q of Electrically Small Antennas" *IEEE Transactions on Antennas and Propagation*, Vol. 44, No. 5, May 1996, pp. 672-676.

[9] H.F. Pues and A.R. van de Capelle, "An impedance-matching techniques for increasing the bandwidth of microstrip antennas," *IEEE Transactions on Antennas and Propagation*, Vol. AP-37, No. 11, November 1989, pp 1345-1354.

[10] IEEE, *IEEE Standard Definitions of Terms for Antennas*, IEEE STD-145, 1993.

[11] D. M. Pozar, *Microwave Engineering*, John Wiley Sons, Inc., 1998, 716 p.

[12] J. Ollikainen and P. Vainikainen, *Design and bandwidth optimization of dual-resonant patch antennas*, Helsinki University of Technology, Radio Laboratory publications, Report S 252, Espoo 2002, Finland, 41 p.

[13] H.W. Bode, *Network Analysis and Feedback Amplifier Design*, Van Nostrad, N.Y., 1945.

[14] R.M. Fano, "Theoretical Limitation on the Broad-Band Matching of Arbitrary Impedances," *Journal of the Franklin Institute*, vol. 249, January 1950, pp. 57-83, and February 1950, pp. 139-154.

[15] J. Ollikainen, *Design and implementation techniques of wideband mobile communication antennas*, Doctoral thesis, Helsinki University of Technology, Radio Laboratory, Espoo, Finland, November 2004.

[16] J. Villanen, P. Vainikainen, "Optimum Dual-resonant Impedance Matching of Coupling Element Based Mobile Terminal Antenna Structures," *Microwave and Optical Technology Letters*, Vol. 49, No. 10, October 2007, pp. 2472-2477.

[17] M. Valtonen, J. Virtanen, *Passiiviset suodattimet*, Yliopistopaino, Helsinki, 2004, 318 p.

[18] http://www.zeland.com (cited 12.3.2008)

[19] P. Vainikainen, J. Ollikainen, O. Kivekäs and I. Kelander, "Resonator-based analysis of the combination of mobile handset antenna and chassis", *IEEE Transactions on Antennas and Propagation*, Vol. 50, No. 10, October 2002, pp. 1433-1444.

[20] J. Villanen, *Compact antenna structure for mobile handsets*, Master's thesis, Espoo, Helsinki University of Technology, February 2003, 83 p.

[21] C.T. Famdie, W.L. Schroeder, and K. Solbach, "Numerical Analysis of Characteristic Modes on the Chassis of Mobile Phones", *Proceedings of EuCAP 2006 European Conference on Antennas & Propagation*, Nice, France, 6-10 November 2006, CD-ROM SP-626 (92-9092-937-5), paper: PA1 345145ct.pdf.

[22] J. Villanen, J. Ollikainen, O. Kivekäs, and P. Vainikainen, "Coupling element based mobile terminal antenna structures", *IEEE Transactions on Antennas and Propagation*, vol. 54, no. 7, pp. 2142 - 2153.

[23] J. Villanen *Miniaturization and Evaluation Methods of Mobile Terminal Antenna Structures*, Doctoral thesis, Helsinki University of Technology, Radio Laboratory, Espoo, Finland, November 2007.

[24] J. Villanen, M. Mikkola, C. Icheln, and P. Vainikainen, "Radiation characteristics of antenna structures in clamshell-type phones in wide frequency range", *Proceedings of the 65th IEEE Vehicular Technology Conference (VTC2007-spring)*, Dublin, Ireland, April 2007, CD-ROM (ISBN 1-4244-0266-2), pp. 382-386.

[25] J. Villanen, J. Poutanen, C. Icheln, and P. Vainikainen, "A wideband study of the bandwidth, SAR and radiation efficiency of mobile terminal antenna structures," *Proceedings of IEEE iWAT 2007 Small Antennas and Novel Metamaterials*, Cambridge, UK, March 2007, pp. 49-52.

[26] J. Poutanen, *Interaction between mobile terminal antenna and user*, Master's thesis, Helsinki University of Technology, Radio Laboratory, Espoo, Finland, September 2007.

[27] J. Poutanen, J. Villanen, C. Icheln, and P. Vainikainen, "Behavior of mobile terminal antennas near human tissue at a wide frequency range," *Proceedings of IEEE iWAT 2008 Small Antennas and Novel Metamaterials*, Chiba, Japan, 2008, paper: P123.

[28] M. Cabedo-Fabres, E. Antonino-Daviu, A. Valero-Nogueira, and M. Ferrando-Bataller, "Wideband radiating ground plane with notches," *Proc. IEEE Antennas and Propagation Society International Symposium Digest*, Washington, USA, July 2005, pp. 560-563.

[29] K.-L. Wong, Y.-W. Chi, B. Chen and S. Yang, "Internal DTV antenna for folder-type mobile phone," *Microwave and Optical Technology Letters*, vol.48, no.6, June 2006, pp. 1015-1019.

[30] J. Holopainen, J. Villanen, C. Icheln, P. Vainikainen, "Mobile terminal antennas implemented using direct coupling," *Proceedings of EuCAP 2006 European Conference on Antennas & Propagation*, Nice, France, 6-10 November 2006, CD-ROM SP-626 (92-9092-937-5), paper: OA17 349858jh.pdf.

[31] ACE Deliverable: *Small Antenna Contest Report*, 31.12.2007.

[32] D. Manteuffel, M. Arnold, "Considerations for Reconfigurable Multi-Standard Antennas for Mobile Terminals," *Proceedings of IEEE iWAT 2008 Small Antennas and Novel Metamaterials*, Chiba, Japan, 2008, paper: P127.

[33] J.D. Kraus, R.J. Marhefka, *Antennas for All Applications, Third Edition*, McGraw-Hill, New York, 2002, pp. 938.

[34] P. Hannula, *Planning parameters for DVB-T portable indoor reception*, Diploma thesis, Espoo, Helsinki University of Technology, Radio Laboratory, February 2004.

[35] EICTA: Mobile and Portable DVB-T/H Radio Access - Interface Specification, version 2.0, 2007.

[36] DVB Project, *DVB-H Implementation Guidelines*, DVB Document A092 Rev. 2 May 2007, http://www.dvb.org -> Standards & Technology (cited 25.3.2008).

[37] http://www.pulsefinland.com/ -> Products and Solutions (cited 1.2.2008)

[38] Z.D. Milosavljevic, "A Varactor-Tuned DVB-H Antenna," *IEEE iWAT 2007 Small Antennas and Novel Metamaterials*, Cambridge, UK, March 2007, pp. 124-127.

[39] L. Huang, P. Russel, "Tunable Antenna Design Procedure and Harmonics Suppression Methods of the Tunable DVB-H Antenna for Mobile Applications," *European Conference on Wireless Technologies*, Munich, Germany, October 2007, pp. 304-307.

[40] M. Komulainen, M. Berg, H. Jantunen, E. Salonen, "Compact varactor-tuned meander line monopole antenna for DVB-H signal reception," *Electronic Letters*, Vol. 43, no. 24, November 2007, pp. 1324-1326.

[41] J. Holopainen, J.Villanen, M. Kyrö, C. Icheln and P. Vainikainen, "Antenna for handheld DVB terminal", *Proceedings of IEEE iWAT 2006 Small Antennas and Novel Metamaterials*, New York, USA, 6-9 March 2006, CD-ROM (ISBN 0-7803-9444-5), p077.

[42] http://www.fractus.com/main/fractus/mob_tv/ (cited 4.2.2008)

[43] http://www.aplac.com/ (cited 20.2.2008)

[44] http://www.semcad.com (cited 28.3.2008)

[45] S. Gabriel, R.W. Lau, and C. Gabriel, "The dielectric properties of human body tissues: III. Parametric models for the dielectric spectrum of tissues," *Physics in Medicine and Biology*, vol. 41, 1996, pp. 2271-2293.

[46] J. Holopainen, J. Poutanen, C. Icheln, and P. Vainikainen, "User effect of antennas for handheld DVB terminal," *Proceedings of ICEAA 2007 International Conference on Electromagnetics in Advanced Applications*, Turin, Italy, 17-21 September 2007, CD-ROM (1-4244-0767-2), paper: 313.pdf.

[47] T. Taga, "Analysis for mean effective gain of mobile antennas in land mobile radio environments," *IEEE Transactions on Vehicular Technology*, Vol. 39, No. 2, May 1990, pp. 117-131.

[48] J. Rahola, J. Ollikainen, "Analysis of isolation of two-port antenna systems using simultaneous matching," *Proceedings of EuCAP 2007 European Conference on Antennas & Propagation*, Edinburg, UK, 11-16 November 2007, paper: ThPA.016.

[49] P. Talmola, "Hand Held Devices and Preferred Spectrum", *Multiradio Multimedia Communications 2005*, Berlin, Germany, 13-17 January 2005, http://mmc05.hhi.de/downloads.html (cited 12.3.2008).

[50] V. Rambeau, H. Brekelmans, M. Notten, K.R. Boyle and J. van Sinderer, "Antenna and input stages of a 470 - 710 MHz silicon TV tuner for portable applications", *Proceedings of European Solid-State Circuit Conf. (ESSCIRC)*, September 2005, pp. 239-242.